國立交通大學

電機學院　電子與光電學程

碩 士 論 文

雙頻帶放大器與陷波濾波器用於WLAN及 WiMAX

Dual-band LNA with notch filter for WLAN and WiMAX

研究生：徐培翔

指導教授：郭建男 教授

中 華 民 國 九十九 年四月

雙頻帶放大器與陷波濾波器用於WLAN及 WiMAX

Dual-band LNA with notch filter for WLAN and WiMAX

研究生: 徐培翔 Student: Hsu Pei-Hsiang

指導教授: 郭建男 Advisor: Chien-Nan Kuo

國 立 交 通 大 學

電機學院　電子與光電學程

碩 士 論 文

A Thesis

Submitted to College of Electrical and Computer Engineering

National Chiao Tung University

in partial Fulfillment of the Requirements

for the Degree of

Master of Science

in

Electronics and Electro-Optical Engineering

June 2010

Hsinchu, Taiwan, Republic of China

中華民國 九十九年四月

雙頻帶放大器與陷波濾波器用於WLAN及 WiMAX

學生 : 徐培翔　　指導教授 : 郭建男 教授

國立交通大學 電機學院　電子與光電學程碩士班

摘要

近年來由於無線通訊的發達，頻段的使用也愈趨頻繁，相對，隨之而來的問題也漸漸浮現，最明顯就是訊號干擾。必須在接收器前端電路設計上，避免系統靈敏度受干擾而大幅降低。通常在接收器前端使用帶通濾波器(Band-pass filter, BPF)降低干擾訊號強度。此外，LNA 會加入增益控制功能，來避免靈敏度受干擾而大幅降低。

對於多頻段多模整合系統，仍必須處理相近頻段干擾之嚴重問題。例如在台灣已經流行之 WLAN（2.4~2.5GHz）及正極力推動之 Wimax（台灣 2.5~2.7GHz）由於信號頻段過於相近，幾乎可以說是重疊，隨之而來的干擾是可以相像的，只有 BPF 無法處理。所以類似的問題將是未來需要研究解決的方向。

所以本論提出了以 Active Notch filter 的方式，來解決二個頻率過於接近的問題，並利用 Varactor 來調整 LC tank，這樣一來可以使得 RFout 可以得到 WLAN or Wimax 的訊號。

Dual-band LNA with notch filter for WLAN and WiMAX

Student : Hsu Pei-Hsiang Advisor : Chien-Nan Kuo

Degree Program of Electrical and Computer Engineering

National Chiao Tung University

ABSTRACT

Because of the advances of wireless communications in recent years, utilization of radio frequency bands has become more and more frequent. As a result, some issues arise gradually, especially the problem of signal interference. Therefore, it is necessary to avoid loss of system sensitivity to interferences by careful receiver front-end circuitry design. Usually band-pass filter (BPF) is used in receiver frontend to suppress interfering signal strength. Also, LNA provides gain control to avoid loss of sensitivity due to interferences.

For multi-band and multi-mode integrated systems, adjacent band interference is another server problem that needs to be addressed. For example, in Taiwan, the already popular WLAN (2.4~2.5GHz) and emerging WiMAX (2.5~2.7GHz), because of the close and almost overlapping frequency bands, it is clear that the signal interference

problem cannot not be handled by only the BPF. This kind of issues point out new research directions.

In this thesis, active notch filter is proposed to resolve issues caused by two signals that are not close in frequency. Also, varactor is utilized to adjust the LC tank such that WLAN or WiMAX signal can be obtained at RF output.

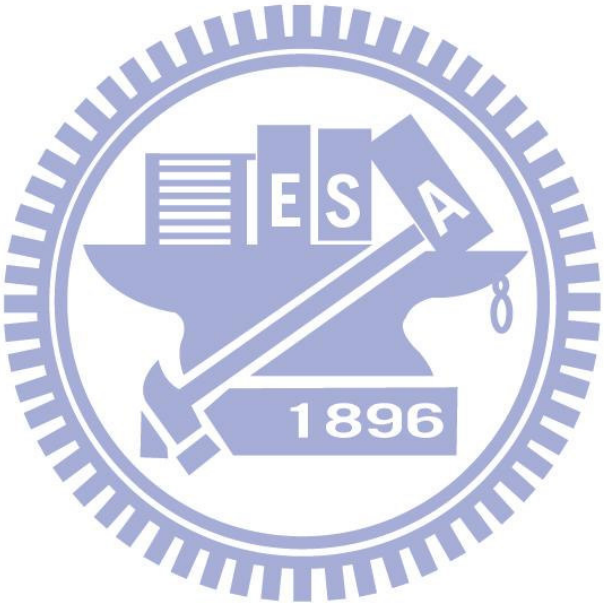

誌　謝

能夠完成畢業論文，順利取得碩士學位，要感謝的人真的很多。首先是，我的父母親，能夠提供我一個沒有經濟負擔的環境一路往上念，並且適時關心我。再來，我要對我的指導教授至上誠摯的感謝。這兩年來，不僅提供了良好的研究環境與設備，並且讓我對射頻及類比電路的領域有深層的了解。適時的指點迷津，讓我學習到有邏輯的分析方法與嚴謹的研究態度。此外我要對昶綜與宗男兩位學長致上萬分的謝意，除了教導我許多軟體與硬體上的使用，也時常分享寶貴的研究與人生經驗，讓我一直有學習的好榜樣。

感謝實驗室的其他學長姐，俊興、燕霖、淑惠、明清、鴻源、鈞琳的不吝指教與技術支援。感謝一起奮鬥一起研究的好同學，煥昇，以及建忠、子超、俊豪、信宇、俊毅、瑋琪、佑偉、宇航等學弟，你們使實驗室不再是一個無聊的地方。

徐培翔

九十九年四月

CONTENTS

TABLE CAPTIONS

FIGURE CAPTIONS

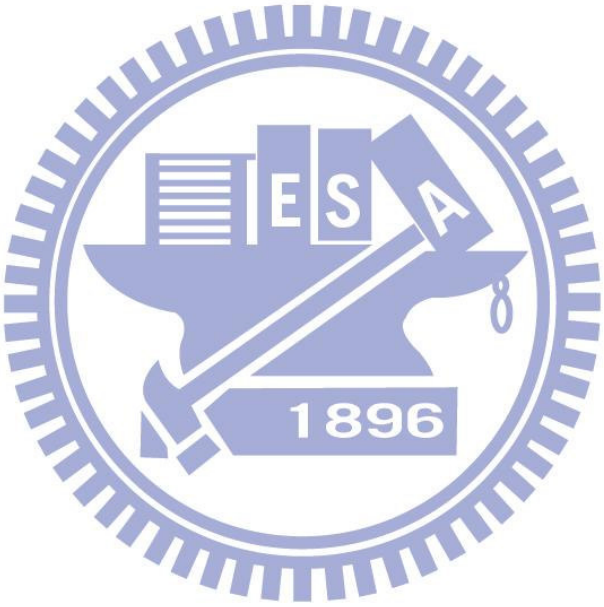

Chapter 1

Introduction

1.1 Motivation

With recent development in the wireless telecommunications sector, frequency ranges are increasingly intensified. Thus problems begin to emerge with signal-to-interference degradation being the most urgent. For example, the next-generation wireless networking WLAN (2.4~2.5GHz), which applies the same modulation scheme (OFDM) as the current mainstream WLAN (2.4~2.5GHz) does in Taiwan, exhibits remarkable anti-interference. However, since both of them use OFDM modulation, the frequency ranges are so close to each other as overlap that frequency interference between adjacent ranges may occur. Likely issues are to be addressed in future studies. Normally, passive comments are used for BPF design. Thus filter circuits with sharp cutoff are necessary to remove adjacent frequency range interference. However, the circuit design may be too complicated since sharper cutoffs entail higher-order circuits. Moreover, the switching-based frequency filtering technique discussed in this study further complicates BPF design. Therefore, in this study, a new idea is proposed which merges LNA and Active notch filter to achieve band selection. A third-order notch filter is utilized instead of a high-order BPF while cross-coupling is adopted to enhance the Q value.

In addition to the above mentioned adjacent frequency interference, strong signal has been identified as another issue. Sensitivity is stressed so much in current LNA design that LNA saturation might occur. Yet current solution to the problem relies so heavily on external circuit that production costs become too high and reliability appears questionable. Thus a gain control method, which determines optimal gain based on control line to selection, is developed in this study.

The two issues discussed above, adjacent frequency interference and strong signal, are needed to be addressed immediately, yet LNA product that supports either filter or gain control is not available in market. Thus a solution is presented in this paper.

1.2 Thesis organization

The paper mainly focuses on LNA gain control and active notch filter.

Chapter 2 presents fundamental LNA design, noise model, gain control circuit and S21 band selection.

Chapter 3 introduces a notch filter which offers very sharp cutoff, yet only applicable to WiMAX signal with a Wp(signal)>Wz(rejection) circuit. Thus a new circuit needed to be provided in order to accommodate Wp(signal)<Wz(rejection). Through merging Wp(signal) >Wz(rejection) and Wp(signal)<Wz(rejection) circuits and using the cross-coupling circuit to enhance Q value, optimal filtering is achieved.

Chapter4, the active notch filter in Chapter3 is used along with S21band selection of Chapter2 to filter WLAN or WiMAX. Moreover, the gain control circuit also provides three gain modes for selection to WLAN or WiMAX.

Chapter 2

The Fundamentals in LNA design

2.1 Introduction

It is well known that low noise amplifier is a fundamental building block in radio frequency (RF) circuit design (Fig 2.1). It amplifies very small RF signal and suppresses the noises contributed by itself to the circuit. The structure of a low noise amplifier is usually simple due to the low noise requirement and the desire for low-power portable systems. However, the design of such a simple circuit, especially with CMOS technology at high frequency, has never been an easy task because it is a compromise of many aspects such as impedance matching, power gain, linearity, and noise performance. In addition to the various design considerations, the lossy substrate of CMOS circuits and the high frequency effects of parasitic components complicate the design problems so that the design targets are hardly achieved or the design process is time-consuming. This is because the parasitic components and the substrate coupling network couple with different parts of the circuit such that accurate design is difficult. Based on the above reasons, we can expect that any modification to the design of a low noise amplifier would invoke design iterations.

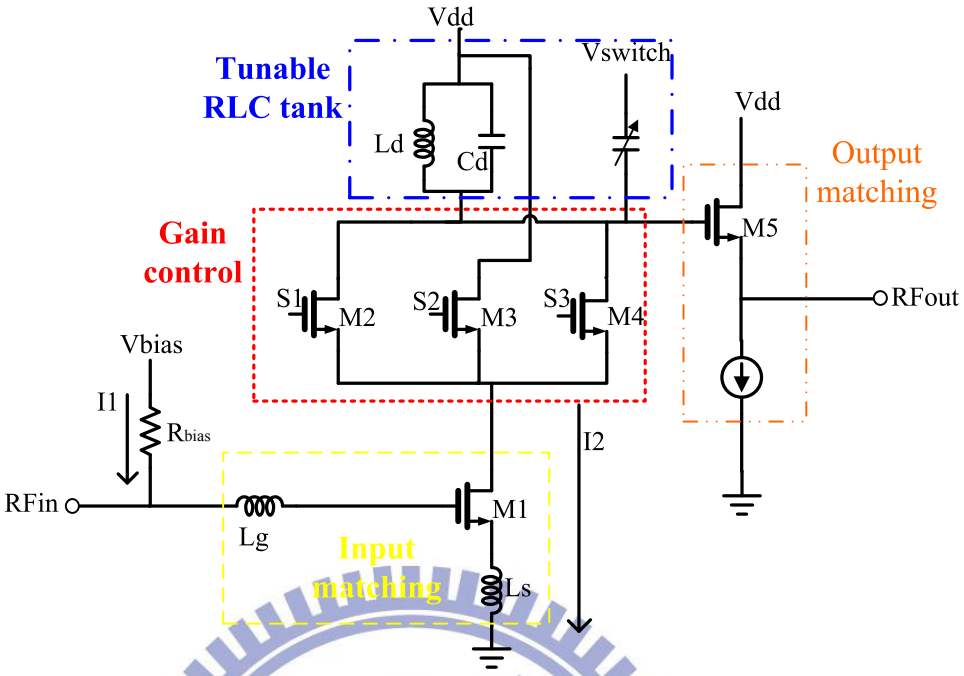

Fig 2.1 Low noise amplifier design

2.2 Low Noise Amplifier Topology and Basic

Fig 2.2 Fundamental LNA design

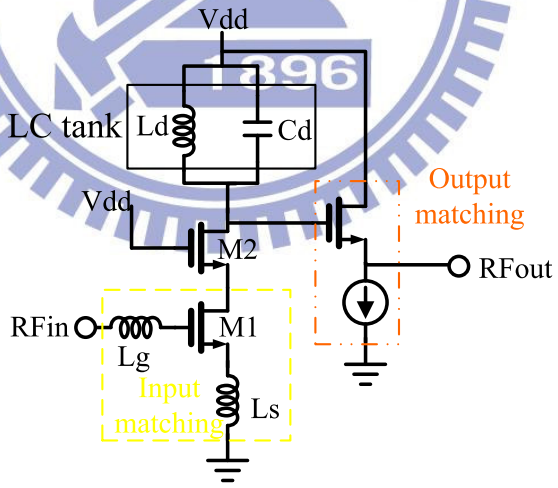

Fig 2.2 Basic of LNA. It was introduced LNA basic design of input matching、output matching、noise model、IIP3 and P1dB

2.2.1 Input matching

In terms of design, centering on 2.55GHz with S11 assigned -20dB, S11 between 2.4~2.7 GHz falls below -15dB. S11 is ideally controlled under -10dB. To accommodate

process variability, however, -15dB is used so that S11 will not exceed -10dB in actual ic test. Fig2.4 shows S11 is below -15dB in the range 2.4~2.7GHz.

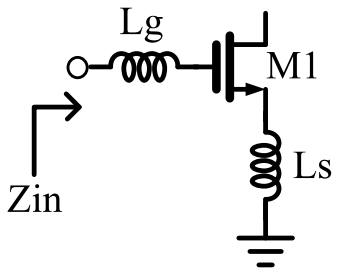

Fig 2.3 inductive degeneration

Fig 2.1 is basic of Low noise amplifier design. Fig 2.3 is desirable to have a narrowband RF signal processing, to get rid of out of band blocker. It employs inductive source degeneration to generate a real term in the input impedance [1] [2]. It offers the possibility of achieving the best noise performance of any architecture. That will describe in following sub-section.

$$Zin = S(Lg + Ls) + \frac{1}{SCgs} + \frac{gm}{Cgs}Ls \qquad (2\text{-}1)$$

$$Zin = \frac{gm}{Cgs}Ls \quad (at\ resonant) \qquad (2\text{-}2)$$

where *Cgs* is the gate-source capacitance and g*m* is the transconductance of the input transistor M1.

This elegant equation shows that designer source inductance to achieve the required 50Ω resistance at resonant frequency and then tune the gate inductance to cancel the reactance part of the input impedance.

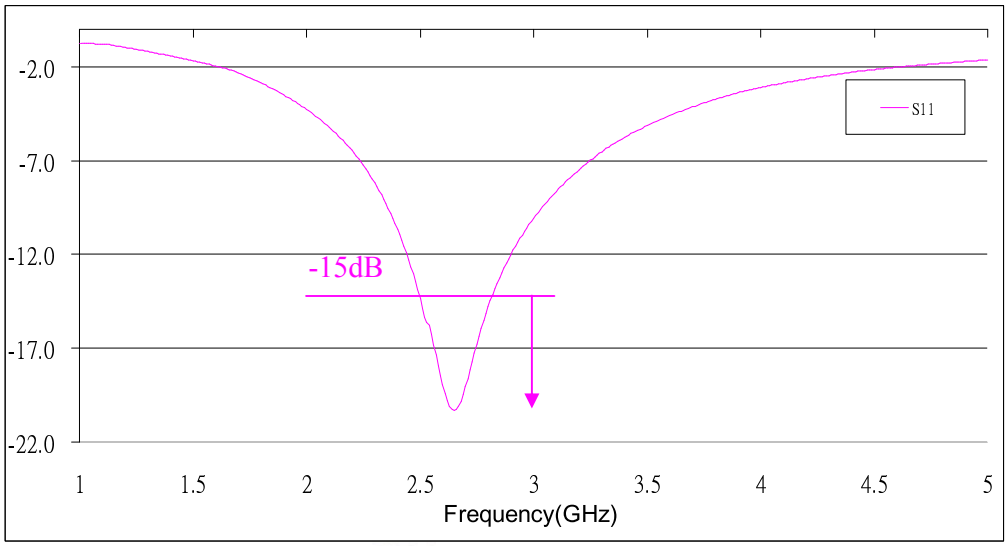

Fig 2.4 Consistently below -15dB for 2.4~2.7GHz.

2.2.2 Noise model

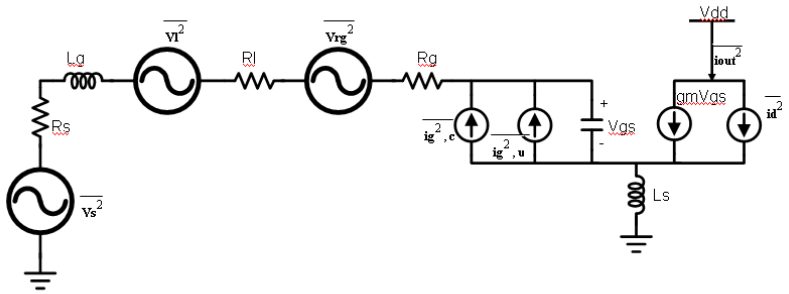

Fig 2.5 Small-signal model for LNA noise model

The noise model [3] [4] can be derived by analyzing the circuit shown in Fig 2.5. Rg is the gate resistance of the NMOS device. The channel thermal noise of the device denotes $\overline{id^2}$. The portion of the total gate noise with and without correlating the drain noise denote $\overline{ig^2,c}$ and $\overline{ig^2,u}$ respectively. The noise factor is defined as

$$F = \frac{Total\_output\_noise}{Total\_output\_noise\_due\_to\_source} \qquad (2\text{-}3)$$

To evaluate the output noise based on driven by a 50Ω source, the transconductance of the input stage is computed first. With the output proportional to the voltage on Cgs, and

noting that the input circuit takes the form of a series-resonant network

$$Gm = gmQin = \frac{gm}{\omega_0 Cgs(Rs + \omega_T Ls)} = \frac{\omega_T}{2\omega_0 Rs} \tag{2-4}$$

The output noise power density due to source Rs is

$$S_{a,src}(\omega_0) = S_{src}(\omega_0) \cdot G_{m,eff}^2 = \frac{4kT\omega_T^2}{\omega_0^2 Rs(1+\frac{\omega_T Ls}{Rs})^2} \tag{2-5}$$

The output noise power density due to Rl and Rg can be expressed as

$$S_{a,Rl,Rg}(\omega_0) = \frac{4kT(R_l + R_g)\omega_T^2}{\omega_0^2 Rs^2(1+\frac{\omega_T Ls}{Rs})^2} \tag{2-6}$$

The noise power density associated with the correlating portion of the gate noise to drain noise can be expressed as

$$S_{a,id,ig,c}(\omega_0) = \kappa S_{a,id}(\omega_0) = \frac{4kT\gamma\kappa gd0}{(1+\frac{\omega_T Ls}{Rs})^2} \tag{2-7}$$

where

$$k = \frac{\delta\alpha^2}{5\gamma}|c|^2 + \left[1 - |c|Q_L\sqrt{\frac{\delta\alpha^2}{5\gamma}}\right]^2 \tag{2-8}$$

$$Q_L = \frac{\omega_0(Ls+Lg)}{Rs} = \frac{1}{\omega_0 RsCgs} \tag{2-9}$$

$$\alpha = \frac{gm}{gd0} \tag{2-10}$$

The power spectral density of un-correlating gate noise and drain noise is derived as

$$S_{a,ig,u}(\omega_0) = \xi S_{a,id}(\omega_0) = \frac{4kT\gamma\xi gd0}{(1+\frac{\omega_T Ls}{Rs})^2} \tag{2-11}$$

where $$\xi = \frac{\delta\alpha^2}{5\gamma}(1-|c|^2)(1+Q_L^2) \tag{2-12}$$

The noise contribution of the drain noise comes from the first device M1 proportional to $S_{a,id}(\omega_0)$. Hence, it is convenient to define contribution of M1 as

$$S_{a,M1}(\omega_0) = \chi S_{a,id}(\omega_0) = \frac{4kT\gamma\chi gd0}{(1+\frac{\omega_T Ls}{Rs})^2} \tag{2-13}$$

where $$\chi = \kappa + \xi = 1 - 2|c|\sqrt{\frac{\delta\alpha^2}{5\gamma}} + \frac{\delta\alpha^2}{5\gamma}(1+Q_L^2) \tag{2-14}$$

Thus the modified noise factor of the device is shown as

$$F = 1 + \frac{R_l}{R_s} + \frac{Rg}{Rs} + \gamma\chi gd0Rs(\frac{\omega_0}{\omega_T})^2 \tag{2-15}$$

by factoring out Q_L

$$gd0Q_L = \frac{gm}{\alpha}\frac{1}{\omega_0 RsCgs} = \frac{\omega_T}{\alpha\omega_0 Rs} \tag{2-16}$$

The noise factor can be re-expressed as

$$F = 1 + \frac{R_l}{R_s} + \frac{R_g}{R_s} + \frac{\gamma}{\alpha}\frac{\chi}{Q_L}(\frac{\omega_0}{\omega_T}) \tag{2-17}$$

The equations show that χ proportional to Q_L^2. The noise factor is proportional to χ over Q_L. Thus a minimum F exists for a particular Q_L.

2.2.3 Vgs selection for IIP3 and P-1dB

A MOSFET linearization technique [5] based on optimum gate biasing is investigated at RF. A novel bias circuit is proposed to generate the gate voltage for zero 3rd-order nonlinearity of the MOSFET transconductance. A MOSFET can also be linearity by biasing at a gate-source voltage (V_{gs}) at which the 3rd-order derivative of its dc transfer characteristic is zero($V_{gs} \approx 0$). One of the major drawbacks of this technique is that a significant IIP3 improvement occurs in a very narrow V_{gs} range (about 10-20mV) around the optimum voltage and there are no known bias means to automatically generate this voltage. Therefore, a bias circuit has to be manually tuned to this voltage, which makes IIP3 to vary significantly with process and temperature variations.

Consider a common-source MOSFET biased in saturation. Its small-signal output

current(Fig 2.6) can be expanded into the following power series in terms of the small-signal gate-source voltage *vgs* around the bias point [6]

$$id(Vgs) = g_1 Vgs + g_2 Vgs^2 + g_3 Vgs^3 + \cdots \tag{2-18}$$

where $g1$ is the small-signal transconductance and the higher-order coefficients ($g2$, $g3$ etc.) define the strengths of the corresponding nonlinearities.

$$A_{IP3} = \sqrt{\frac{4}{3}\left|\frac{g_1}{g_3}\right|} \tag{2-19}$$

The power series coefficients generally depend on the dc gate-source and drain-source voltages, V_{gs} and V_{ds}.

$$g_1(V_{GS}) = \frac{\partial id}{\partial V_{GS}}$$
$$g_2(V_{GS}) = \frac{1}{2}\frac{\partial^2 id}{\partial V_{GS}^2} \tag{2-20}$$
$$g_3(V_{GS}) = \frac{1}{6}\frac{\partial^3 id}{\partial V_{GS}^3}$$

The results are presented in Fig. 2.7. As can be seen, in the transition region from moderate to strong inversion, there is a *Vgs* at which $g_3 = 0$ and $A_{IP3} = \infty$.

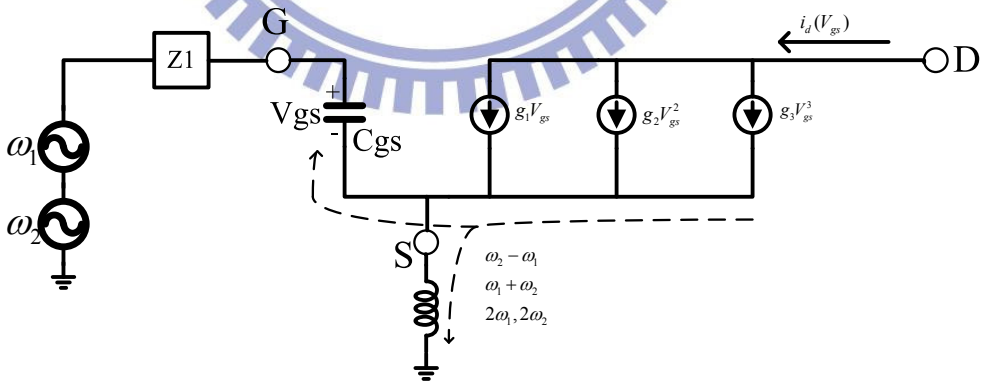

Fig 2.6 Small-signal nonlinear equivalent circuit of a common-source MOSFET

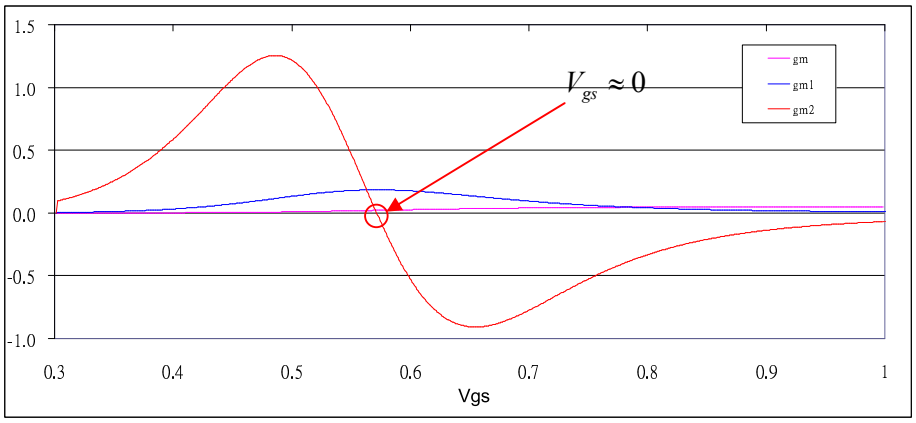

Fig 2.7 gm2 vs Vgs($V_{gs} \approx 0$)

2.2.4 Output matching

Output matching was using source follower. Zout= 50Ω

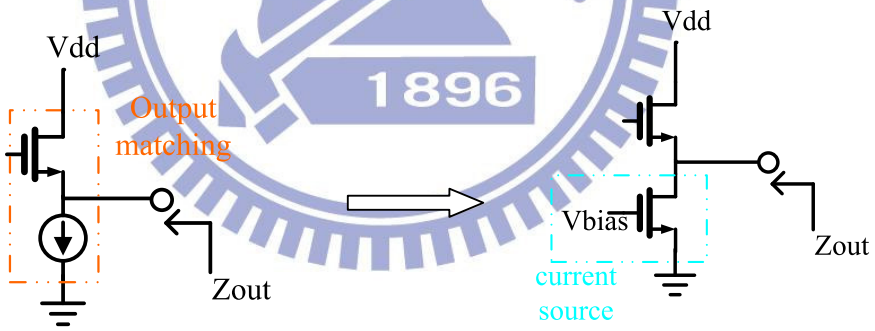

Fig 2.8 Source follower to output matching

S22 between 2.4~2.7GHz is consistently below -10dB as the output buffer suggests

2.3 Gain control

The low noise amplifiers (LNA) should have low noise figures to increase sensitivity of the receivers, and high linearity to prevent interference from undesired adjacent-channe1 signals [7] [8]. To increase dynamic range of the receivers and to reduce linearity required of the downconversion mixers, the LNA is required to provide variable gain. When the RF input power is large, the gain of the LNA should be reduced.

The electric resistance based gain control dose produce a lower NF under high gain、medium gain or low gain [9]. However, the complexity in mathematical calculations and resistance shifts (maximum 20%) always restrict its design. Finally, another approach was adopted out of consideration for circuit stability, namely current splitting [9]. Being a straightforward approach, one need only to adjust the size of MOSFET to determine medium gain or low gain, yet a higher NF is expected due to change in current.

LNA gain can be controlled in discrete steps by current splitting as shown in Fig 2.9. Transistors M1, M2, M3 and M4, form a common-emitter transconductance stage which converts the RF input power into current. Transistor M3、M4 form current switch.

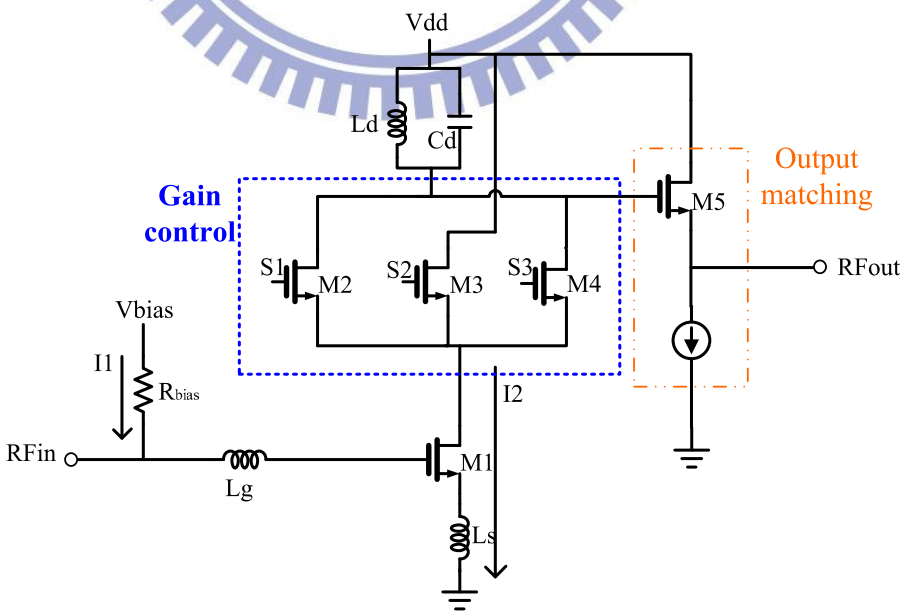

Fig 2.9 LNA of Gain control circuit of current splitting. It was using current splitting design.

This method has using current splitting to change gain step. But, it has high noise figure at low gain mode.

In the high-gain mode (Fig 2.10 High gain mode Is1=I2) all output current of the transconductance stage is injected into M2.

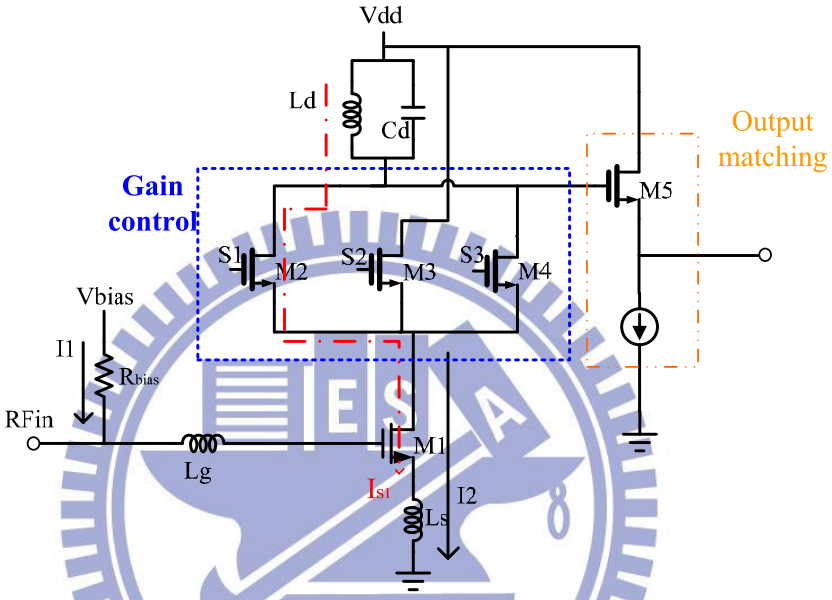

Fig 2.10 High gain mode Is1=I2

In middle-gain mode (Fig 2.11 Medium gain mode Is1+Is2=I2) the output currents of M2 and M3 are dumped to the power supply. This reduces LNA gain. In medium-gain mode, only output current of M3 is dumped to the power supply. In this gain-control scheme, the gain steps between successive gain modes depend on the device size ratios of M2, M3.

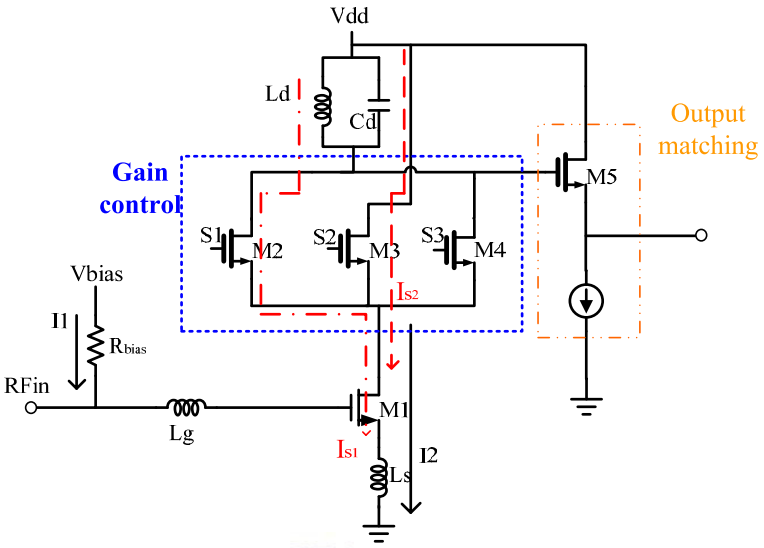

Fig 2.11 Medium gain mode Is1+Is2=I2

In low-gain mode (Fig 2.12 Low gain mode Is2+Is3=I2) the output currents of M3 and M4 are dumped to the power supply. This reduces LNA gain. In medium-gain mode, only output current of M3 is dumped to the power supply. In this gain-control scheme, the gain steps between successive gain modes depend on the device size ratios of M2, M3 and M4.

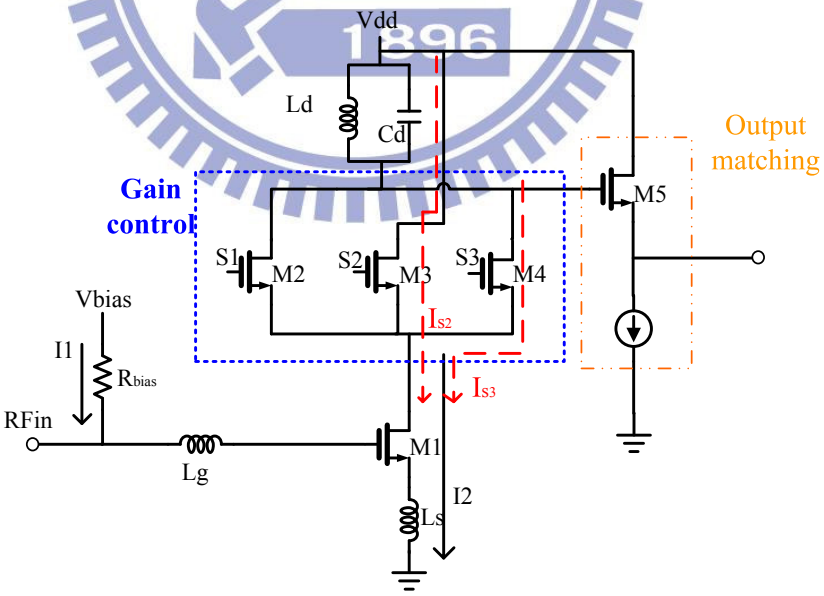

Fig 2.12 Low gain mode Is2+Is3=I2

A disadvantage of current-splitting is that the LNA has high noise figures in low-gain modes. The noise figure of a circuit measures the degradation of signal-to-noise ratio (SNR)

caused by the circuit. Dumping away some of the signal current decreases the signal power, and hence degrades the noise figure by reducing the SNR at the LNA output. Another way to view this noise-figure degradation phenomenon is that the input-referred noise voltage of M1 is amplified by an un-degenerated differential-pair transconductance stage formed by Ml, M2, M3and M4. In some applications, little noise-figure degradation is allowed in the LNA low gain modes. The reason is that the interference levels increase when the desired signal power increases. To have large signal-to-noise- plus-interference ratio (SNIR), the noise figures of the LNA in the low-gain modes should remain low to allow margin for handling interference. The I_1 and I_2 is a current mirror. That support LNA a stable current source. Because, the gain control circuit is a change current circuit. Base on current source, the LNA will be a stable when using gain control function.

Table 2.1 Switch table of gain control.

Control	High Gain	Middle Gain	Low Gain	
S1	1	1	0	1：1.8 V 0：0 V(gnd)
S2	0	1	1	
S3	0	0	1	

The setting result can reference Fig 2.14、Fig 2.15、Fig 2.16

2.4 Tunable RLC Tank

The frequency tuning is achieved by the first order RLC tank, as show in Fig 2.13. Thus we could derive the impedance as below. [10]

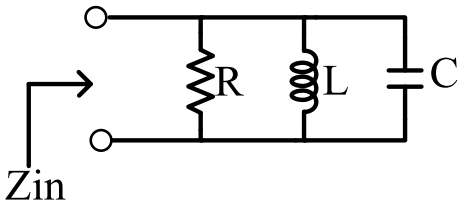

Fig 2.13 RLC tank. It was using varactor to change LC tank and change frequency range apply to WLAN and WiMAX

$$Zin(j\omega) = \left[\frac{1}{j\omega L} + j\omega C + \frac{1}{R}\right]^{-1} \quad \left(\omega_0 = \frac{1}{\sqrt{LC}}, Q = \frac{R}{\omega_0 L} = \omega_0 RC\right)$$

$$\cong \left(\frac{1}{j(\omega_0 + \Delta\omega)L} + j(\omega_0 + \Delta\omega)C + \frac{1}{R}\right)^{-1} \quad (\text{Let } \omega = \omega_0 + \Delta\omega)$$

$$\cong \left(\frac{\frac{1}{j\omega_0 L}}{1 + \frac{\Delta\omega}{\omega_0}} + j(\omega_0 + \Delta\omega)C + \frac{1}{R}\right)^{-1} \quad \left(\text{use } \frac{1}{1+x} \approx 1 - x + \cdots\right)$$

$$\cong \left(\frac{1}{j\omega_0 L} - \frac{\frac{\Delta\omega}{\omega_0}}{j\omega_0 L} + j\omega_0 C + j\Delta\omega C + \frac{1}{R}\right)^{-1} \quad \left(\because \omega_0^2 = \frac{1}{LC}\right)$$

$$\cong \left(\frac{1}{R} + 2j\Delta\omega C\right)^{-1} = \frac{1}{\frac{1}{R} + 2j\Delta\omega C}$$

$$\cong \frac{R}{1 + 2j\Delta\omega C} \quad \left(\because RC = \frac{Q}{\omega_0}\right)$$

$$\cong \frac{R}{1 + 2jQ\frac{\Delta\omega}{\omega_0}} \quad (\text{if } R \to \infty)$$

$$\cong \frac{1}{j2C\Delta\omega} \quad (\text{C is varactor}) \tag{2-21}$$

In this design, frequency tuning is achieved by a tunable LC tank at the output of the common-gate transistor drain. This resonator consists of a fixed-value inductor and a MOS varactor. To obtain frequency tuning from 2.45GHz to 2.6GHz, the value of the capacitance in this work varies from 1.01pF to 1.34pF. The equivalent circuit model of the LC tank is add show in Fig 2.12, including the gate-drain capacitor, Cgd2, of M2 (M3, M4). The resistors R_{ls} and R_{cs} standing for the parasitic of the inductor Ld and the varactor (Cvar), respectively, degrade the quality factor of the resonator. The resonance frequency and the quality factor are therefore determined as

$$\omega_0 = \frac{1}{\sqrt{L_d(C_{gd2} + C_{\text{var}})}} \tag{2-22}$$

$$Q = \frac{R_{lp} \parallel R_{cp}}{\omega_0 L_d} \tag{2-23}$$

where

$$R_{lp} \approx R_{ls} \cdot (Q_L^2 + 1) \quad , \quad R_{cp} \approx R_{cs} \cdot (Q_c^2 + 1) \tag{2-24}$$

$$Q_L = \frac{\omega_0 L_d}{R_{ls}} \quad , \quad Q_c = \frac{1}{\omega_0 R_{cs} C_{\text{var}}} \tag{2-25}$$

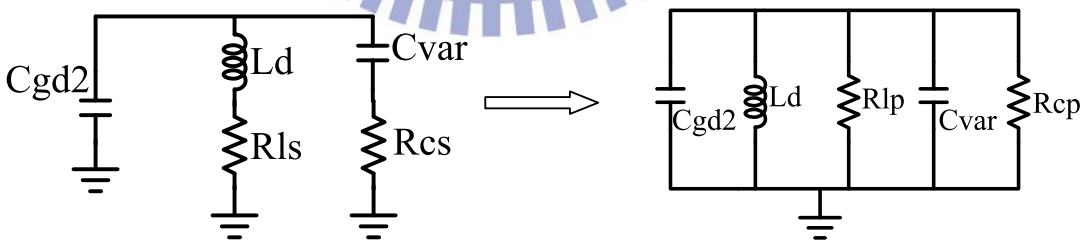

Fig 2.14 The LC tank transformation

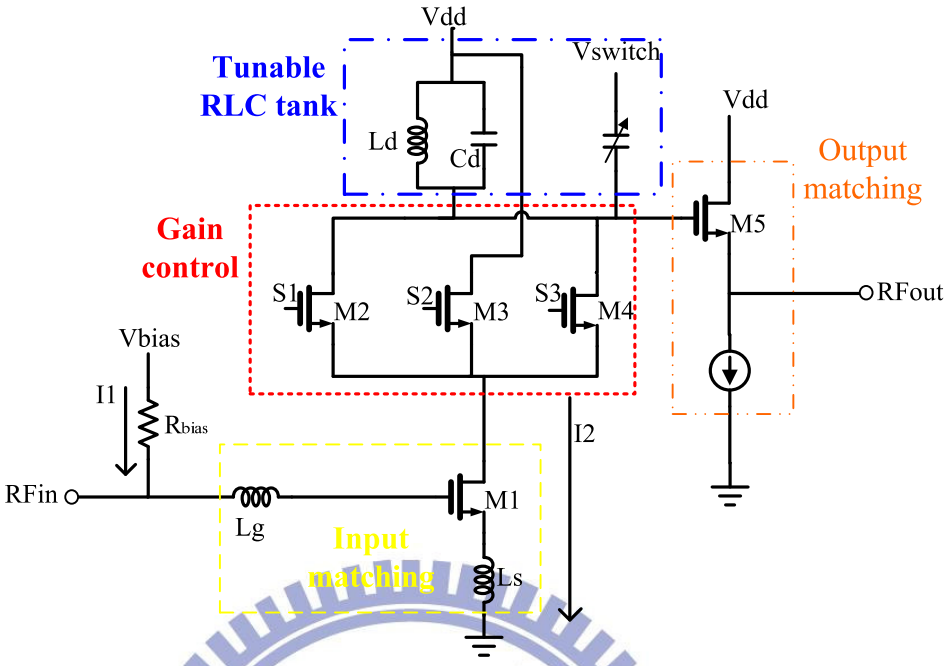

Fig 2.15 Tunable RLC tank circuit of LNA

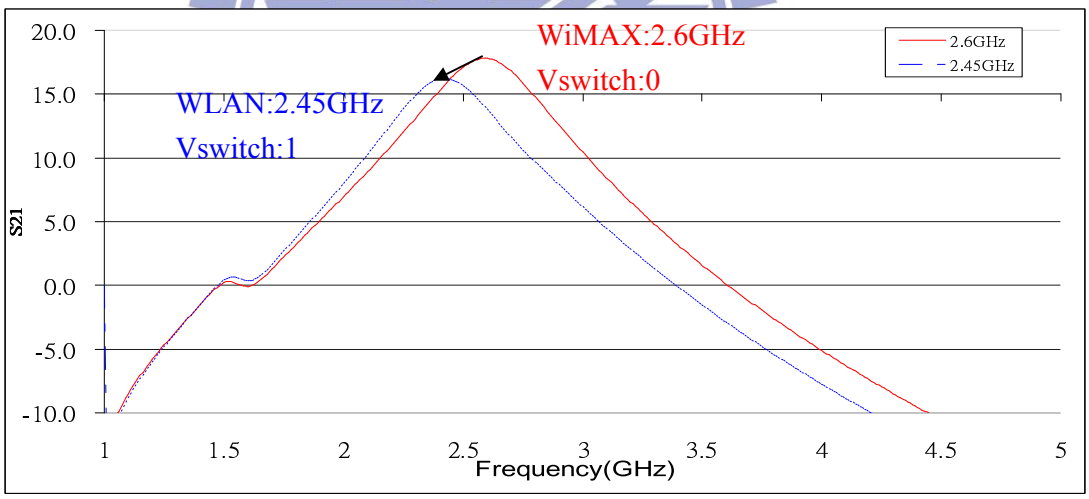

Fig 2.16 Fix L and tunning C

Table 2.2 Vswitch setting

	Band frequency	Vswitch	1：1.8 V 0：0 V(gnd)
A	2.6GHz	0	
B	2.45GHz	1	

As suggested by Table 2.2, one needs only to change the voltage of Vswitch to change S21.

Merging section2.3 and section2.4 a LNA circuit providing both gain control and band-selection can be obtained. The simulated circuit suggests WLAN/ WiMAX can be selected via Vswitch with gain control available. Table 2.3 shows the settings for gain control and band-selection.

Table 2.3 Setting for gain control and band-selection

Frequency	Gain	S1	S2	S3	Vswitch
A、2.6GHz	High	1	0	0	0
	Medium	1	1	0	0
	Low	0	1	1	0
B、2.45GHz	High	1	0	0	1
	Medium	1	1	0	1
	Low	0	1	1	1

Based on the setting in Table 2.3, simulation result for WLAN and WiMAX is obtained, as presented in Fig 2.14、Fig 2.15 and Fig 2.16.

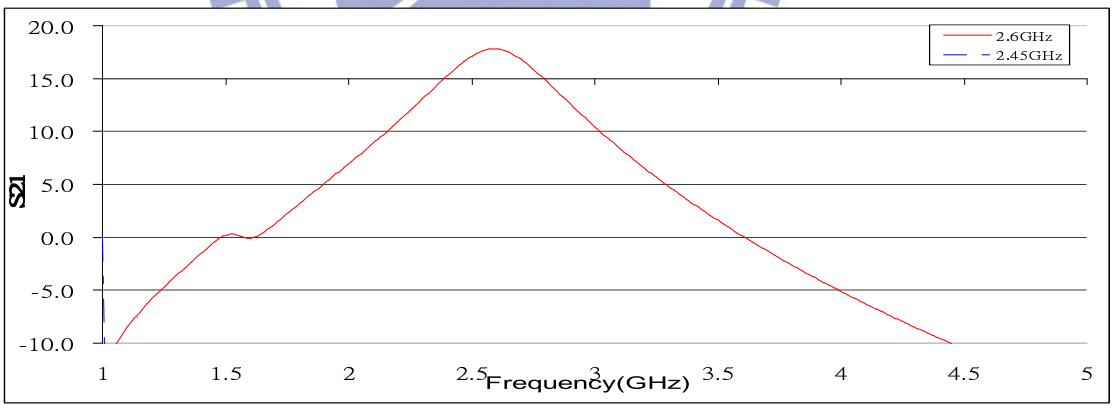

Fig 2.17 S21 High gain

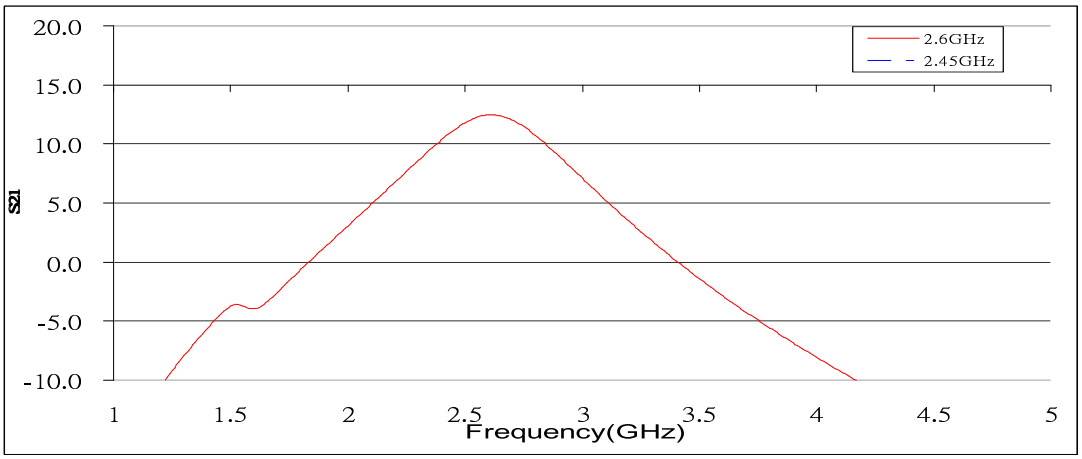

Fig 2.18 S21 Medium gain

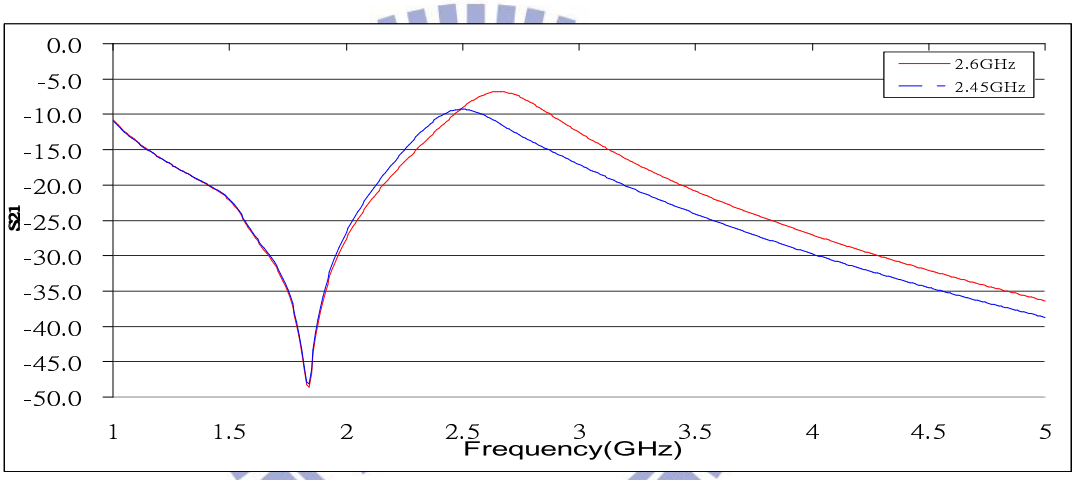

Fig 2.19 S21 Low gain

2.5 Simulation of LNA

Fig 2.17~2.20 presents three gain modes of WLAN and WiMAX in two band frequencies. As shown in Fig 2.17, two band frequencies and three gain modes could be obtained based on the settings in Table 2.3.

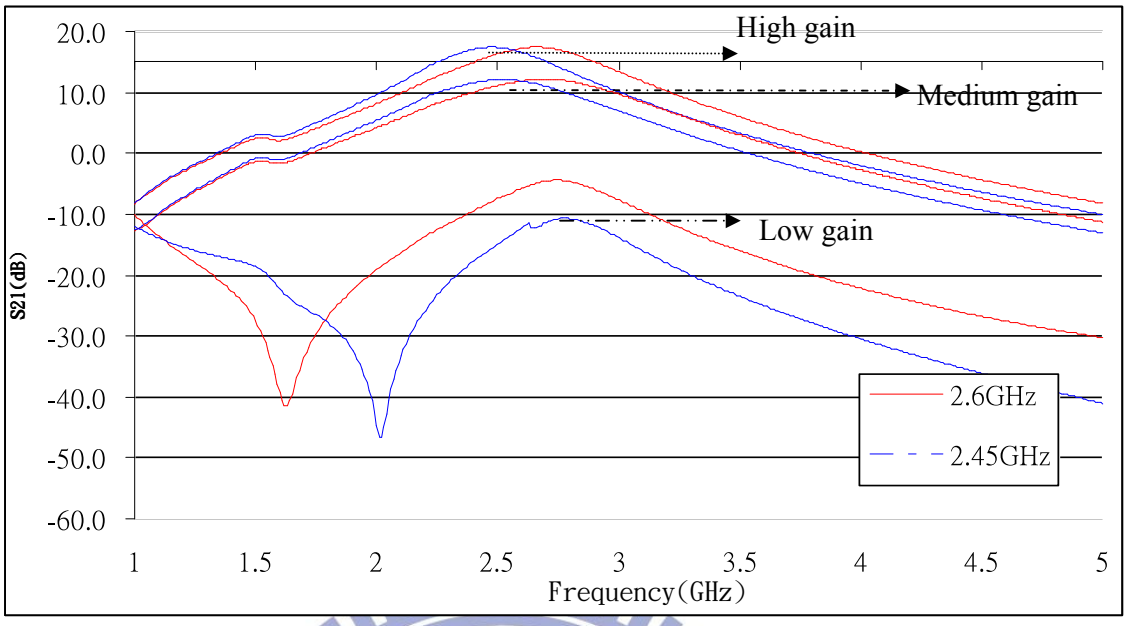

Fig 2.20 Gain control of WLAN and WiMAX of S21

Plotted against three gain modes of WLAN and WiMAX in two band frequencies , S11 is consistently below -10dB as presented in Fig 2.18.

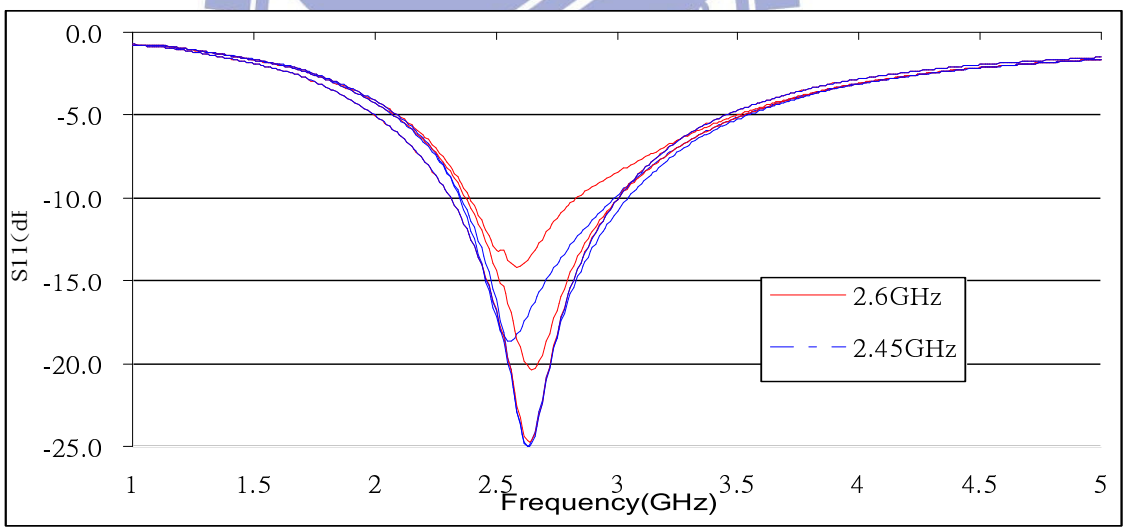

Fig 2.21 WLAN and WiMAX of S11.

Fig 2.19 is an output buffer matching based on output buffer, consistently below -10dB.

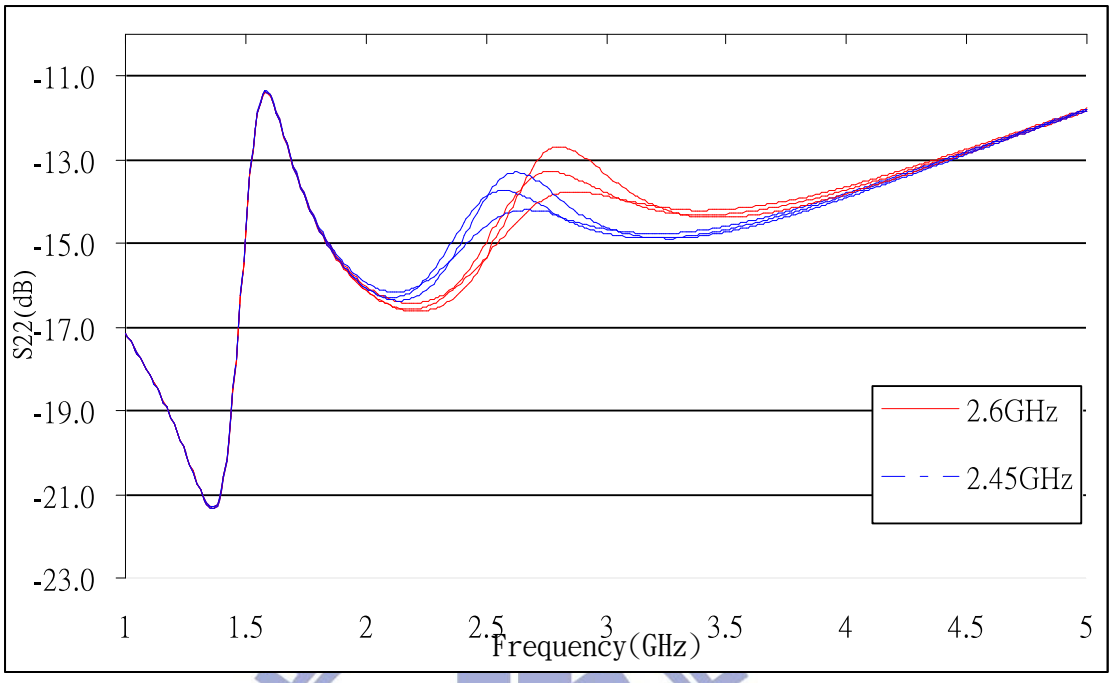

Fig 2.22 WLAN and WiMAX of S22.

It could be found from Fig2.20 low gain mode incurs a considerable NF adopting the gain control approach of current splitting.

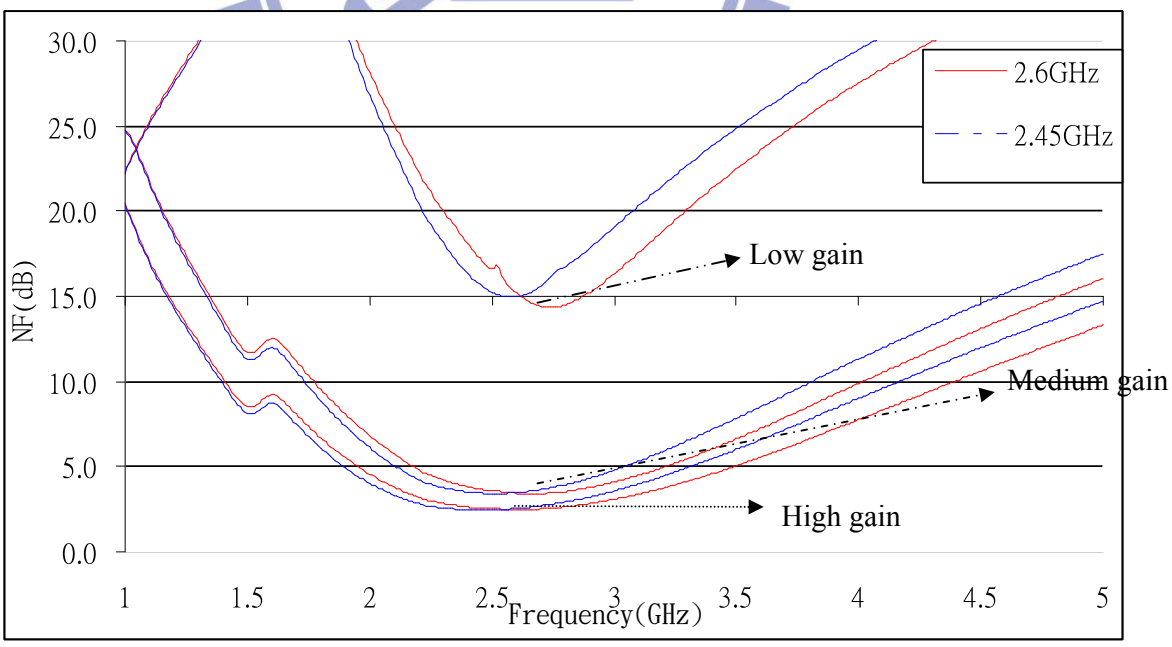

Fig 2.23 WLAN and WiMAX of NF.

Table 2.4 Presents the LNA simulation results, which suggests the two band frequencies

provide similar results based on Vswitch.

Table 2.4 Simulation results of WLAN and WiMAX

	WiMAX			***WLAN***		
	Simulation					
	High gain	Medium gain	Low gain	High gain	Medium gain	Low gain
Technology	0.18um CMOS Standard					
Vdd	1.8V					
S21	17.4	13	-6.6	17.4	12.5	-7.1
S11	-15	-19.7	-21	-14.6	-15	-16.3
S22	-15	-15	-15	-15	-15	-15
NF	2.6	4.3	17.7	2.5	4.3	18.1
P1dB	-22	-16	-3	-21.5	-15.5	-3.5
IIP3	-12.4	-5.8	1.6	-12.1	-6.9	1.1
Power comsumption	13.86mW					

Chapter 3

Active notch filter design

3.1 Introduction

The primary requirements for LNA, gain control and band-selection, have been met in Chapter 2. As a further step, LNA will be so designed as to produce either WLAN or WiMAX signals or. BPF (Band Pass Filter) is the most widely used filter, as well as an ideal one being able to remove noise while retain signal. The disadvantage is that high-order filter, for which the circuit is too complicated to design, is needed when two bands are two close to one another. The target set for this study, rendering band-selection applicable to either S21 or filter, might fail to be met.

Notch filter [11] is adopted out of consideration for the above mentioned issues, since the notch filter used in three-order circuit could produce both Wz and Wp as suggested by simulation. Wz provides a low impedance filter (ideally 0Ω) which removes noise frequencies, while Wp provides a high impedance filter (ideally 0Ω) which clear up the influence of noise on wanted frequencies. The most competitive advantage provided by notch filter is that a smooth curve could be obtained even with third-order circuit, yet third- or fifth-order circuit is necessary to achieve similar result with BPF [12] [13].

The condition ω_p **(signal)>** ω_z **(rejection) [14]** could mostly be satisfied as suggested in the retrievable literature, which provides considerable references. However, the requirements for notch filter are only partially met. Thus another condition ω_p (signal) < ω_z (rejection) has to be taken into consideration. In addition to fully meet the two conditions, ω_p (signal)> ω_z (rejection) and ω_p (signal) < ω_z (rejection), the two circuits should be merged into one with switching circuit incorporated to equip notch filter with band-selection. Uncertainties and errors in process are also considered, for example, effects from PCB power line

Thus a varactor is fitted to notch filter circuit for correction. Previous notch filter was commonly used as an IR filter (Image rejection filter), yet it first acts as an adjacent frequency filter in this study. Thus its impedance matching, negative impedance circuit and power supply, as well as the circuit itself need to be considered. Basically, the circuit of notch filter should satisfy the following conditions:

1、$|Z_{notch}\ (\omega_{rejection})|>|Z_{CG}\ (\omega_{signal})|$

$|Z_{notch}\ (\omega_{rejection})|<|Z_{CG}\ (\omega_{signal})|$

As presented in Fig 3.1

2、adaptable notch frequency.

3、a 10dB difference between it and S21.

4、providing a good Q with the negative impedance

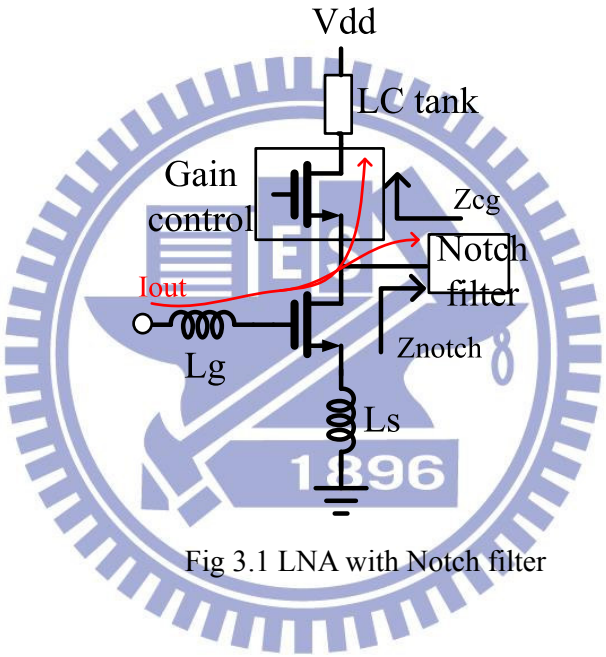

Fig 3.1 LNA with Notch filter

3.2 Notch filter

3.2.1 Series notch filter

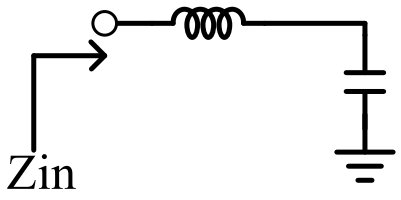

Fig 3.2 Series notch filter

$$\omega_z = \frac{1}{\sqrt{LC}} \quad \text{(Support one zero pole)} \qquad (3\text{-}1)$$

Wanted frequency is liable to be subjected to interference since only a single Wz is available, though first-order notch filter [15] produces good results. The reason for that may be attributed to inappropriate Wz design for first-order circuit. Thus third order notch filter is selected instead, providing mainly Wp and Wz. According to mathematical calculations, the filtered noise would not interfere with the wanted frequency whether Wp>Wz or Wp<Wz .

3.2.2 Third order notch filter: ω_p (signal)> ω_z (rejection)

The third-order active notch filter is based on a series LC resonator (section 3.2.1) that resonates at the image frequency. Fig 3-4 is the third notch filter circuit design, which provides $\omega_p > \omega_z$ [16] [17].

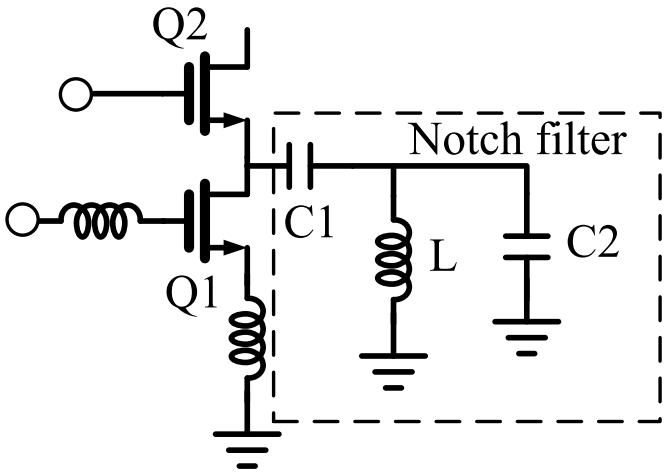

(a)

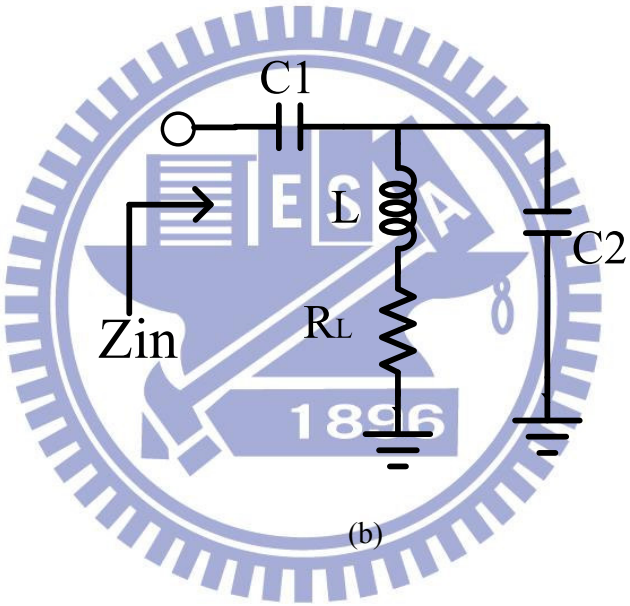

(b)

Fig 3.3 (a) Schematic of the IR LNA with the third-order notch filter.

(b) The filter's equivalent circuit including the series resistance of the on-chip inductor only.

Originally, C1 was a DC block, yet through simulation and mathematical derivation, it was found that change in C1 might produce the same results as a high-order filter does under ideal conditions.(similar to a rectangular filter), (3-2) is mathematical derivation.

$$Z_{in}(S) = \frac{1}{SC_1} + SL \,||\, \frac{1}{SC_2}$$

$$= \frac{1}{SC_1} + \frac{SL \cdot \frac{1}{SC_2}}{SL + \frac{1}{SC_2}}$$

$$= \frac{1}{SC_1} + \frac{S}{1 + S^2 LC_2}$$

$$= \frac{1 + S^2 L(C_1 + C_2)}{SC_1 \cdot (1 + S^2 LC_2)} \qquad (3\text{-}2)$$

So

Pole point: $\omega_p = \frac{1}{\sqrt{LC_2}}$ (3-3)

Zero point: $\omega_z = \frac{1}{\sqrt{L \cdot (C_1 + C_2)}}$ (3-4)

Where Wp>Wz (3-5)

From (3-3)、(3-4), Wp(signal) and Wz(rejection) can be obtained respectively. Wp is codetermined by L and C2, offering a high impedance, which enables the wanted frequency falling on Wp to ensure signal integrity. Wz is determined together by L、C1 and C2, offering a low impedance, which enables the wanted frequency falling on low impedance.

At the image frequency, the impedance looking into the filter can be reduced to zero such that the entire image signal will be extracted from the original path, whereas at the wanted frequency, the input impedance of the proposed filter is maximized. Therefore, the loss of the wanted signal can be avoided. The ability of Wz depends on the difference of impedance between the filter and the original LNA at the image frequency. The larger the difference is, the higher the Wz can be obtained.

The filter can provide low impedance at the image frequency and high impedance at thewanted frequency. This filter is designed not only to reject the image signal, but also to remove the effect of the parasitic capacitance in the signal path of cascade amplifier. Thus, by providing high and low impedance at the wanted and image signals, the filter archives Wz and good noise performance at the same time. However, the major drawback of this filer comes from the quality of the on-chip inductor that affects the overall quality factor of the filter.

Fig 3.4 shows Wz generates a low impedance to remove noise frequency while Wp generates a high impedance to retain WiMAX band. Yet Wp and Wz can be infinitely close to each other though Wp is always greater than Wz. Likewise two advantages could be inferred from (3-3) and (3-4):

1、Change in C1 will never affect WiMAX band.

2、Remarkable sharp cutoff might be achieved.

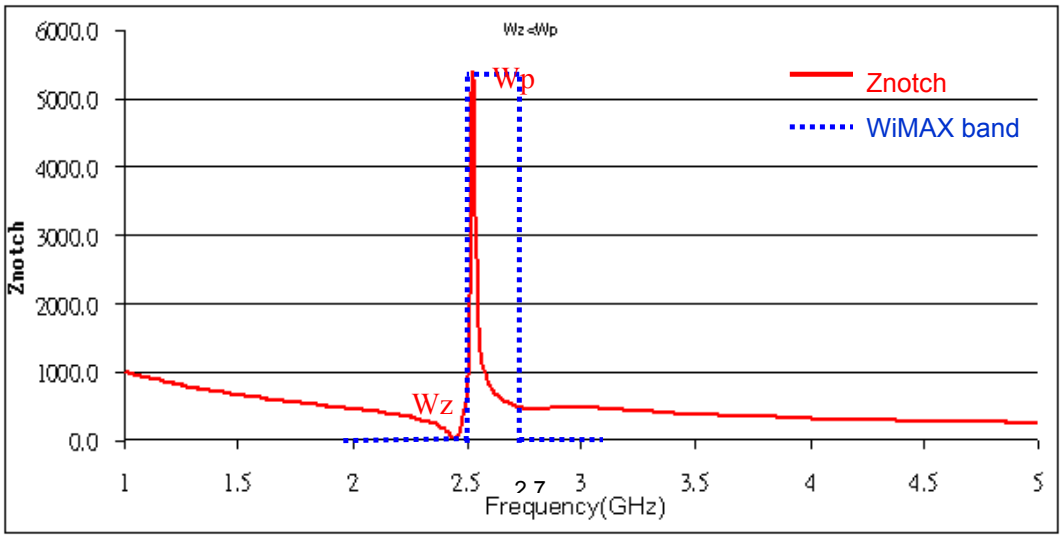

Fig 3.4 Wp>Wz Znotch vs WiMAX band

In typical CMOS technology, the quality factor of the on-chip inductor is dominated by the series resistance. By neglecting all the parasitic components, except the series resistance of the on-chip inductor, the equivalent circuit of only the filter can now be represented as shown in Fig. 3.3(b), where is the series resistance. Also assume that only the quality factor of the

filter at the image frequency is of most interest at this moment; the quality factor of filter is given by Quality factor of filter

$$Q = \frac{(\frac{L_1}{C_1 + C_2})^{1/2}}{R_L} \qquad (3\text{-}6)$$

Filter performance is largely dependent on Q value. However, Q value is usually damped by parasitics from passive components In (3-6), Q value of the circuit is constrained by RL. To bring up Q, a cross-coupling circuit (section 3-3) is fitted.

3.2.3 Third order notch filter: ω_p (signal) < ω_z (rejection)

The constraint condition for WiMAX has been met in section3.2.2. Yet one more issue need to be addressed, that is how to meet the condition for WLAN. Considering the result of section3.2.2, whether Wp<Wz can satisfy the constraint condition for WLAN need to be determined. No circuit constrained by condition Wp<Wz has ever been reported based on retrievable literature. Thus, a new circuit has to be designed so as to meet Wp<Wz.. Yet the new circuit can not differ too much from Wp>Wz circuit, since such a circuit is too complicated to design. Therefore,thea new design should be developed based on improving the design in Fig 3.3 (a). Thus the difference between the two circuits could be narrowed and the circuits could be merged afterwards to spare some component.

If L2 is fitted in Fig 3.3 (a) to turn C1 into a DC block, Wp<Wz could be satisfied, as shown in Fig 3.5

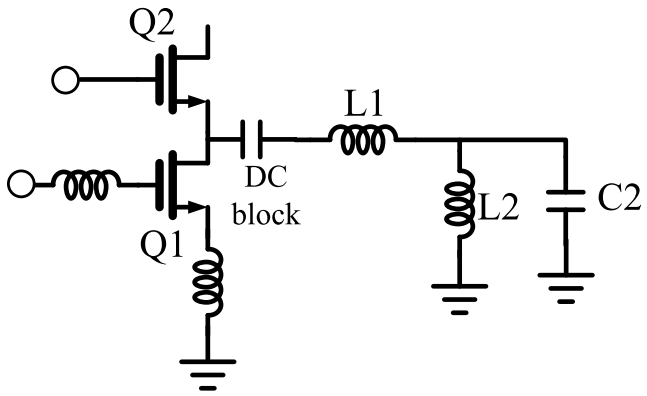

(a)

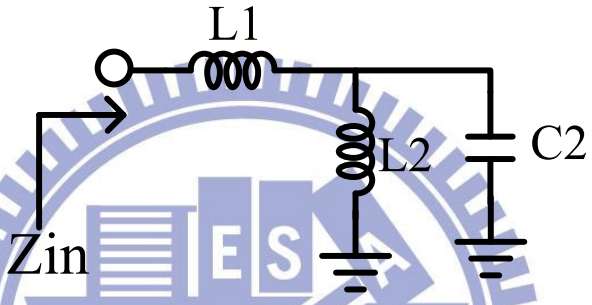

(b)

Fig 3.5 (a) Schematic of the IR LNA with the third-order notch filter.
(b) The filter's equivalent circuit including the series resistance of the on-chip inductor only.

$$Z_{in}(S) = SL_1 + \frac{SL_2 \cdot \frac{1}{SC_2}}{SL_2 + \frac{1}{SC_2}}$$

$$= SL_1 + \frac{SL_2}{1 + S^2 L_2 C}$$

$$= \frac{SL_2 + SL_1 + S^3 L_1 L_2 C_2}{1 + S^2 L_2 C_2}$$

$$= \frac{S[S^2 L_1 L_2 C_2 + (L_1 + L_2)]}{1 + S^2 L_2 C_2} \qquad (3\text{-}7)$$

So

$$\text{Pole point :} \quad \omega_p = \frac{1}{\sqrt{L_2 C_2}} \tag{3-8}$$

$$\text{Zero point :} \quad \omega_z = \frac{1}{\sqrt{(L_1 \,||\, L_2) C_2}} \tag{3-9}$$

where

Wp<Wz

Equation (3-8) and (3-9) are derived (3-7). Wp is still generated by L2 and C2, while Wz is generated by (L1||L2) and C2. Therefore, Wp will never be less than Wz. Likewise, once L1 is determined, Wz can be adjusted. Such method is identical to section 3.2.2; Wp and Wz are again used to generate a sharp cutoff filter.

It could be observed from Fig 3.6 that Wz generate a low impedance to pass noise frequency, Yet the high impedance from Wp can retain WLAN band. Wp and Wz can infinitely approach each other with Wp being never greater than Wz. Likewise, such a design provides two advantages which can be inferred from Equation (3-8) and (3-9).

1、Change in C1 will never affect WLAN band.

2、Providing a very sharp cutoff filter.

Similarly, out of concern for Q value of the circuit as a whole, a cross-coupling circuit is integrated.

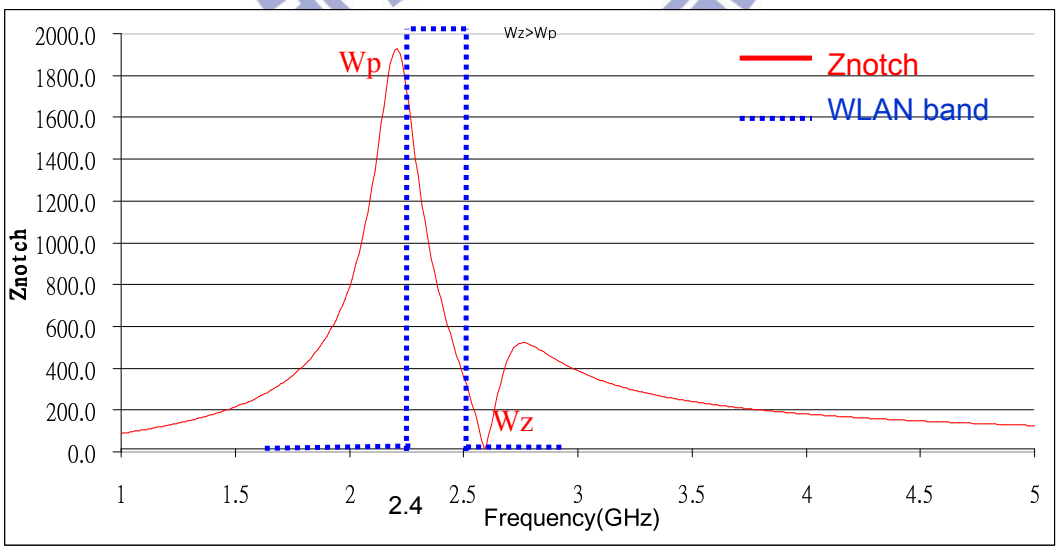

Fig 3.6 Wp <Wz Znotch vs WLAN band

3.3 Cross-coupling circuit

As an important parameter for a filter, Q value determines filter performance. Based on the circuit in section3.2, to bring up Q value damped by parasites, a cross-coupling circuit is introduced.

Negative impedance is utilized to enhance Q value of the circuit. Fig 3.7 shows a cross-coupling circuit of differential [18] [19], which is changed to single mode since single mode circuit is used in this study.

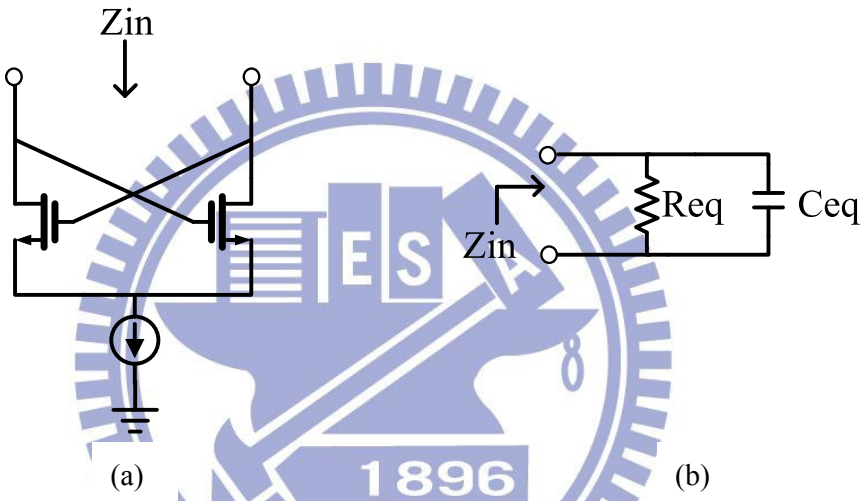

Fig 3.7 (a) Cross-coupling circuit of differential

(b) Equivalent circuit

$$\text{Zin} = R_{eq} \parallel C_{eq}$$

$$= -\frac{2}{gm} \quad \text{(differential circuit)} \qquad (3\text{-}10)$$

Fig 3.8 is the single mode Cross-coupling. Originally the circuit of differential has a double-ended voltage 2V [+V-(-V)], current I, --> double-ended impedance Zin=-2/gm. If –V end is changed to AC GND (connected to VDD) the double-ended voltage turns V [V-0] while the current is invariant.

--> double-ended（single-ended）impedance is $Zin = -\frac{1}{gm}$. (3-11)

In fact, the GND rather than the circuit impedance has changed.

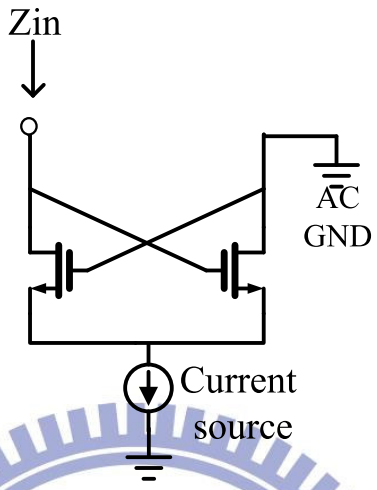

Fig 3.8 single mode Cross-coupling

Cross-coupling circuit provides a good negative impedance circuit, yet it is found during simulation that the electric current needed under different frequencies is variable. Therefore, two power supply sources are available for selection through S6 and S7. Thus different power supply can be generated.

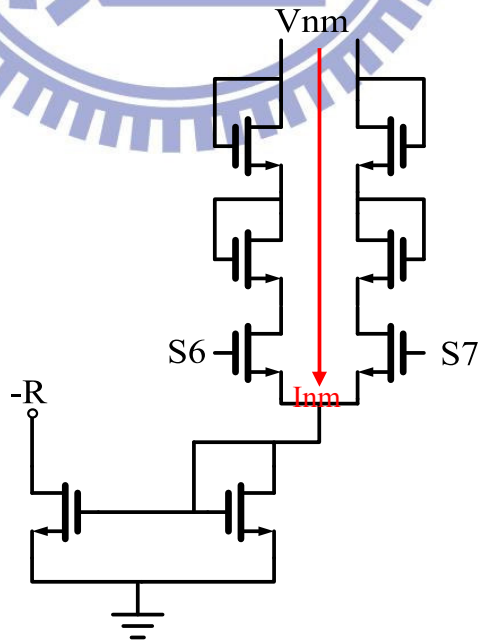

Fig 3.9 Current source of Notch filter

3.4 Active notch filter

Through the circuit design in section3.2 and 3.3, Fig 3.10 may be obtained. However, section3.2.2 and 3.2.3 must be merged as a prerequisite, which offers two benefits：

1、It could be inferred that the most significant differences between the two circuits lies in that section 3.2.3 is equipped with DC block and L1. Apart from that, they have the same components. Thus if switching is integrated into the design, selection function might be available.

2、Varactor is replaced with C2, which is used to modulate the filter so as to accommodate uncertainties or other variables in process.

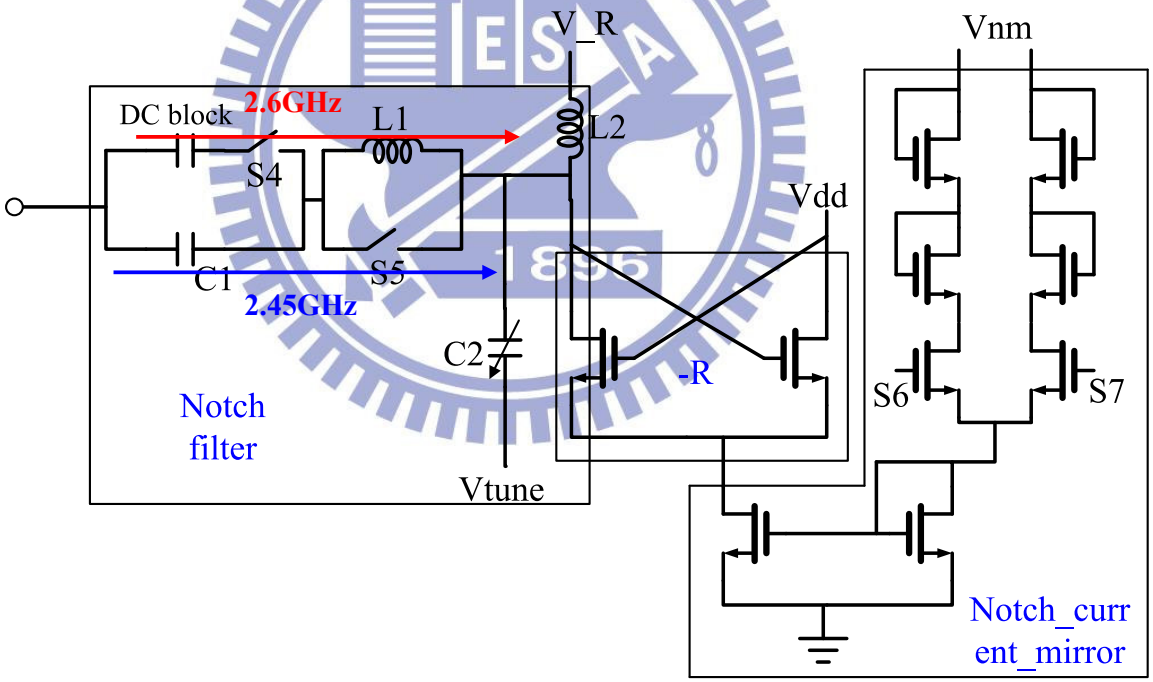

Fig 3.10 Active notch filter

For the active notch filter four-phase switching is adopted. To reduce control lines of pin 0、1, a CMOS inverter design is introduced. Thus the originally expected four control lines are reduced to a single one, greatly mitigate the complexity in control.

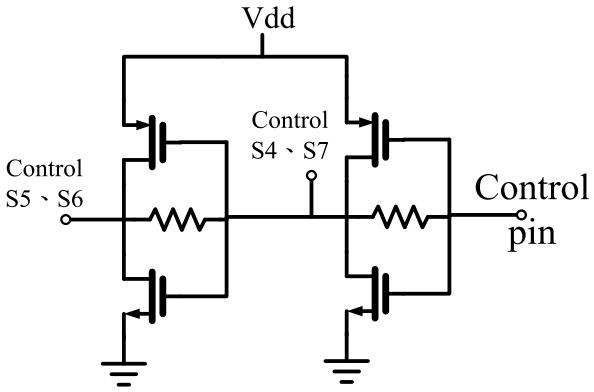

Fig 3.11 CMOS inverter

Table 3.1 Active notch filter switch setting

Notch Frequency	S4	S5	S6	S7		Control pin
A、2.45GHz	0	1	1	0	←	1
B、2.60GHz	1	0	0	1		0

Table 3.1 is the switch setting for active notch filter, A、2.45GHz is the circuit (Wp<Wz) of section 3.2.3. B、2.60GHz is the circuit (Wp>Wz) of section 3.2.2.

Chapter 4

Dual-band LNA and Active notch filter with Measurement

4.1 Dual-band LNA and Active notch filter

Fig 4.1 shows a complete Dual-band LNA with Active notch filter. Firstly, wanted frequency (WLAN or WiMAX) for S21 is determined via a Vswitch, then filter frequency is identified through Control pin 0 or 1. Output wave of WLAN or WiMAX could be produced after such settings, and band selection is achieved. Frequency band is selected based on the setting in Table 4.1.

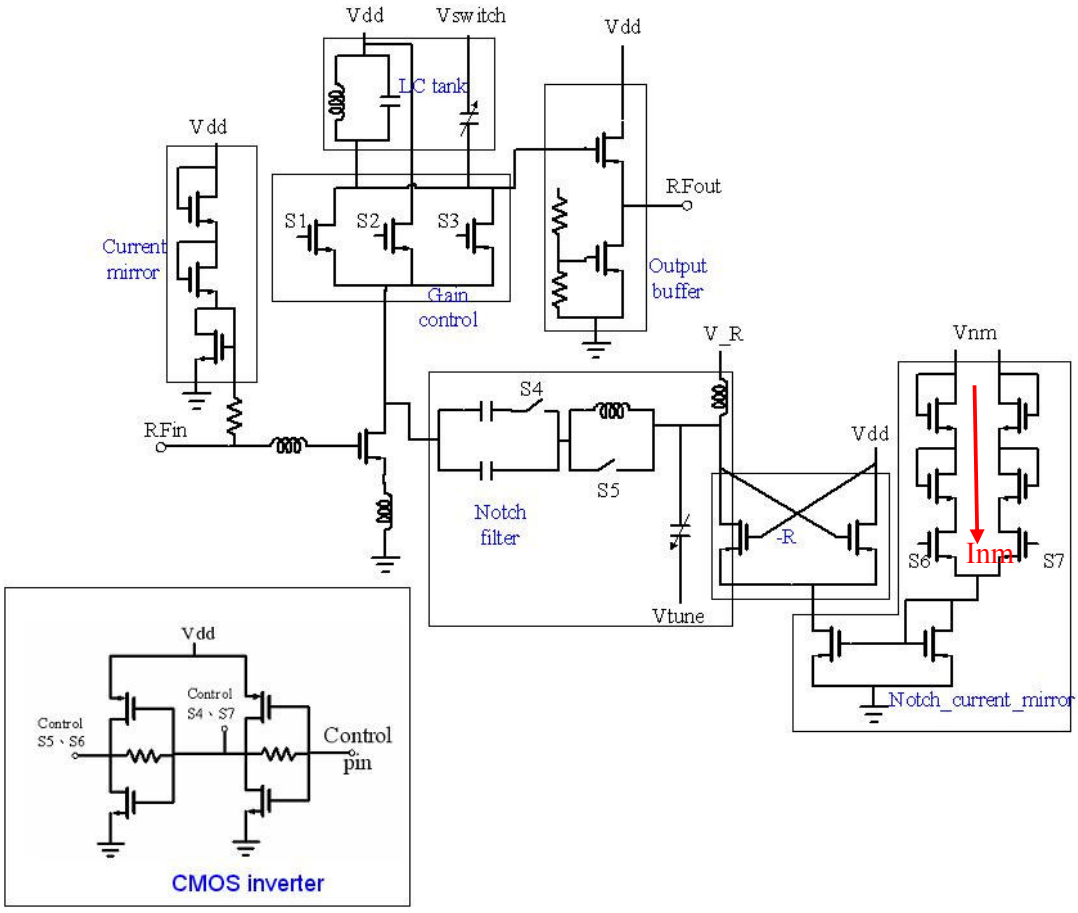

Fig 4.1 Dual-band LNA with Active notch filter

Table 4.1 shows the controls lines needed. The simplification in control lines offers further ease of operation.

Table 4.1 Dual-band LNA with Active notch filter setting

Frequency	Gain	S1	S2	S3	Vswitch	Control pin
A、2.60GHz	High	1	0	0	0	1
	Medium	1	1	0	0	1
	Low	0	1	1	0	1
B、2.45GHz	High	1	0	0	1	0
	Medium	1	1	0	1	0
	Low	0	1	1	1	0

4.2 Measurement

Fig 4.2 shows the comparisons between LNA_simulation, LNA_notch filter_simulation, LNA_notch filter_measurement and WiMAX signal. It could be found from the comparisons that notch filter do provide significant filter performance. Band frequency could be selected through the setting in Table4.1. Filter width falls short of expectations due to design aspects, yet it entails further studies. In LNA_notch filter_measurement a 400MHz shift in frequency as a whole it is found. The reason for that is attributed to the design defects in varactor resulting from using the outdated process data. Further more, as prescribed, when Vtune=0.2v notch frequency corresponds to 2.45GHz, yet Vtune has to be raised up to 0.7v for 2.45GHz.

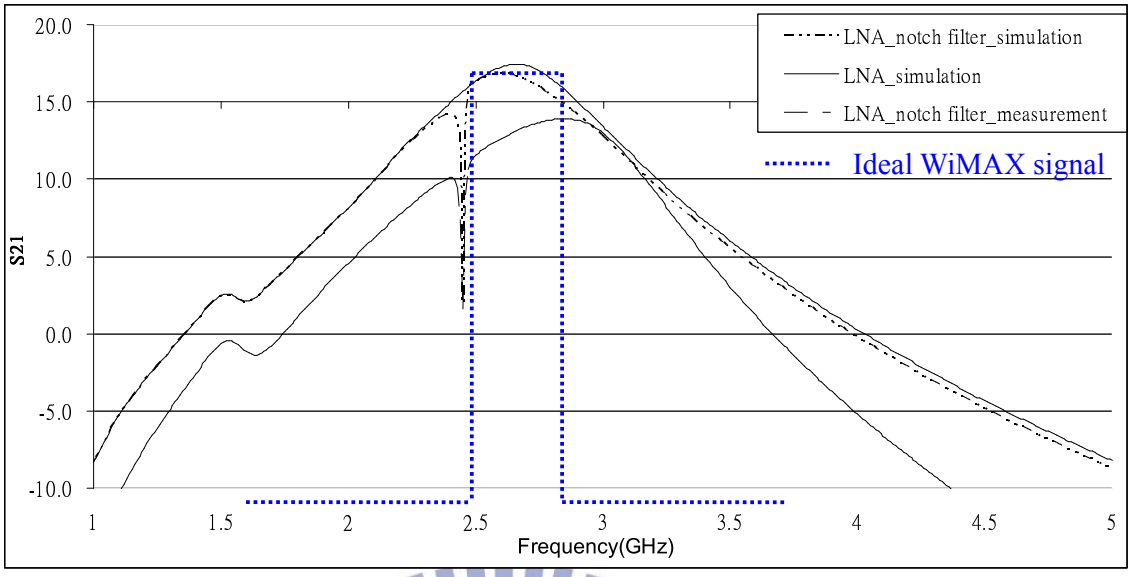

Fig 4.2 simulation and measurement of WiMAX

Fig 4.3 shows the adjustments in Vtune after measurement. Initially notch frequency corresponds to 2.45GHz when Vtune=0.2v. Due to uncertainties in process, the measured notch frequency is 2.53GHz. To bright notch frequency back to 2.45GHz, Vtune voltage is raised up to 0.7v. Where α is the filter frequency width, the greater α better performance, yet it's narrowed down to 100MHz in range.

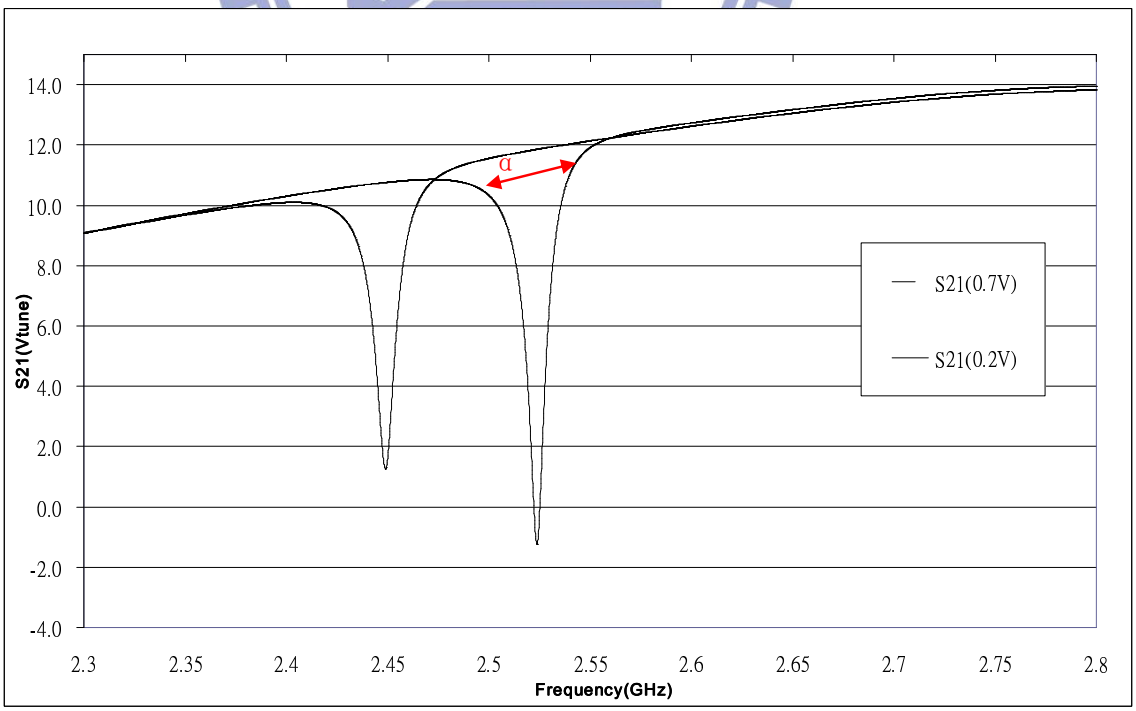

Fig 4.3 Voltage adjustment of Vtune

Fig 4.4 shows the comparisons between LNA_simulation, LNA_notch filter_simulation, LNA_notch filter_measurement, WiLAN signal. It could be found from the comparisons that notch filter do provide significant filter performance. Band frequency could be selected through the setting in Table4.1. Filter width falls short of expectations due to design aspects, yet it entails further studies. In LNA_notch filter_measurement a 400MHz shift in frequency as a whole is found. The reason for that is the same as that for Fig 4.2. Further more, as prescribed, when Vtune=1.3v notch frequency corresponds to 2.6GHz, yet Vtune has to be raised up to 1.8v for 2.6GHz. The reason for that can be attributed to the narrow frequency range which restricts Vtune from reaching the expected frequency.

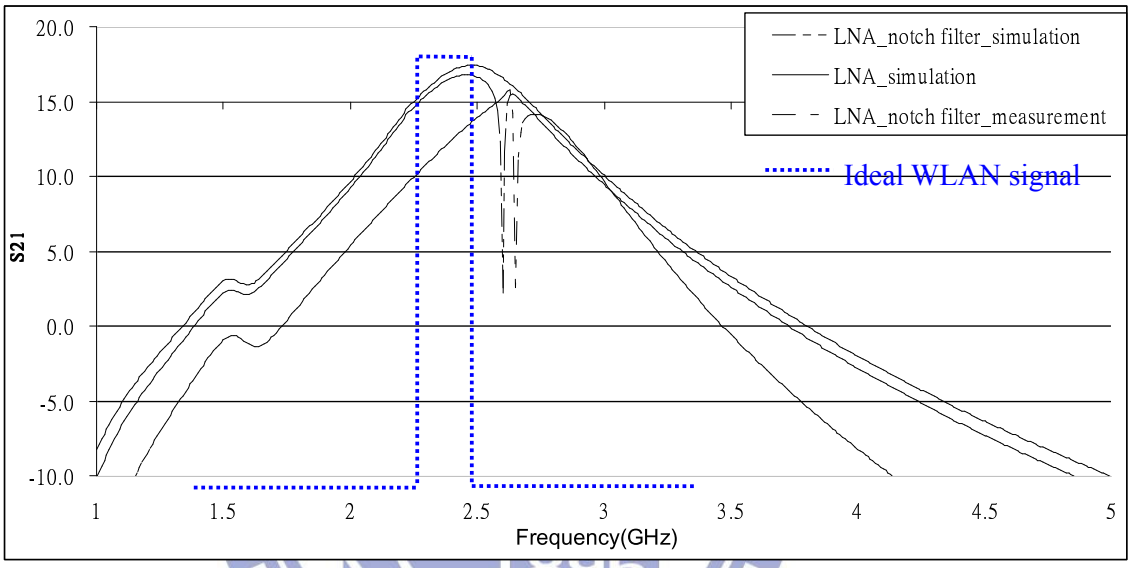

Fig 4.4 simulation and measurement of WLAN

Fig 4.5 shows the adjustments in Vtune after measurement. Initially notch frequency corresponds to 2.6GHz when Vtune=1.3v. Due to uncertainties in process, the measured notch frequency is 2.72GHz. To bright notch frequency back to 2.6GHz, Vtune voltage is raised up to 1.8v, yet only 2.65GHz is reached. Where α is the filter frequency width, the greater α better performance, yet it's narrowed down to 100MHz in range.

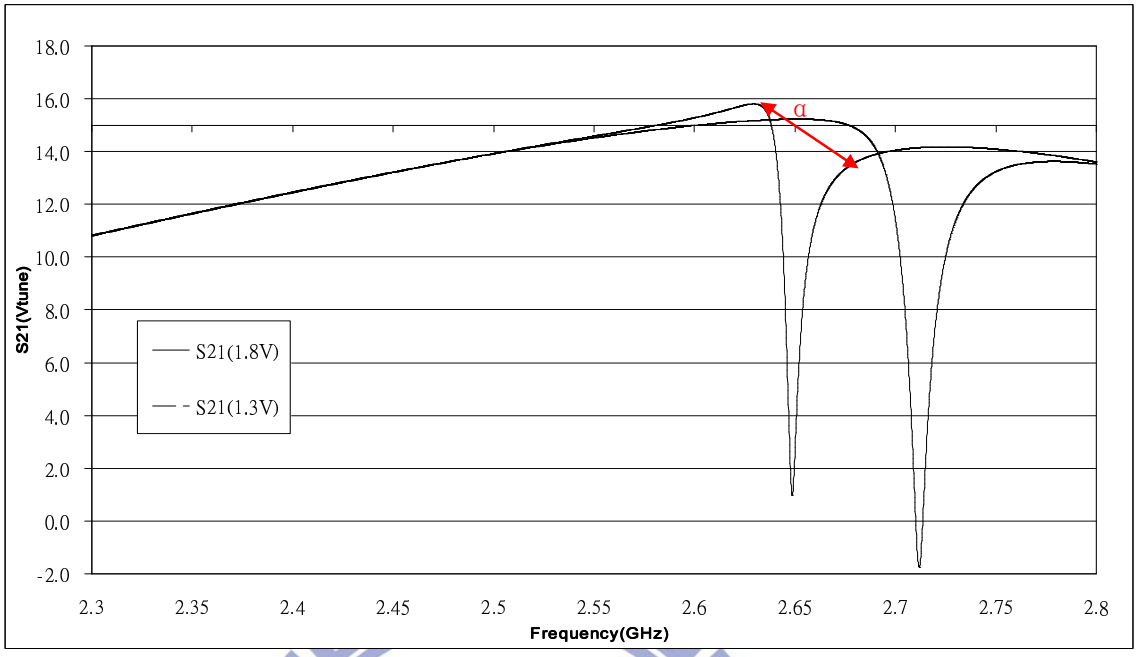

Fig 4.5 Adjustment voltage of Vtune

Fig 4.6 presents the available frequency range for notch filter

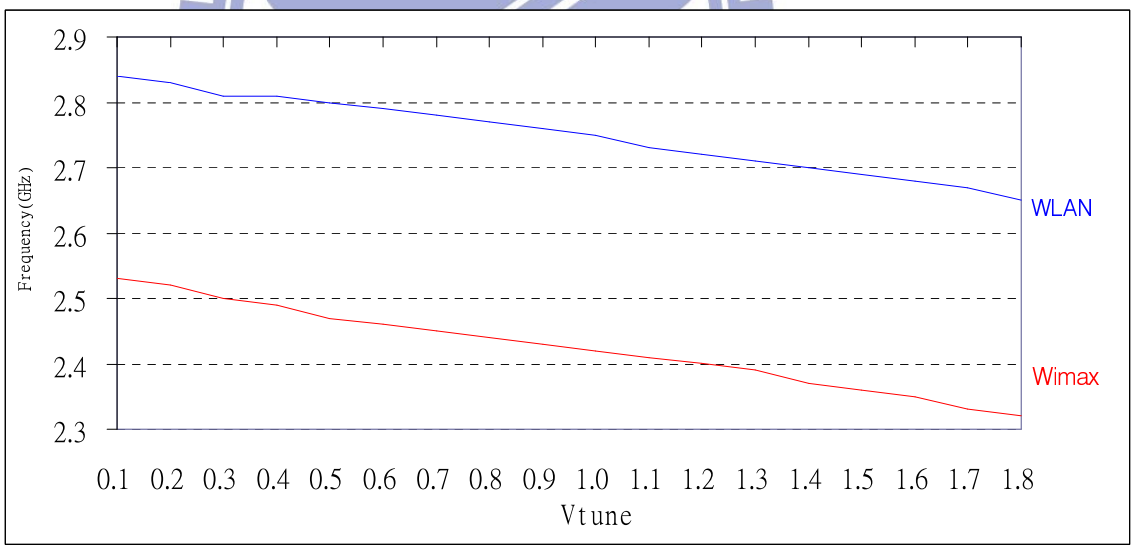

Fig 4.6 Vtune vs frequency of notch filter

4.3 Inm (notch current) vs Notch Q value

In this chapter, a parameter △ is defined at first,

△= center frequency – notch frequency. (4-1)

△ the greater the better filter performance

From Fig 4.7 it could be found △=12.62(2.6GHz)-1.59(2.45GHz)=11.03. While the magnitude of Inm(Fig 4.1) is closely correlated with △. It could be inferred from Fig 4.7, when Inm=525uA, Notch filter acquires an optimal Q value. △ goes down with decreasing Inm. However, if Inm is too large, for example, Inm=545uA, notch filter might vibrate to generate a peak value.

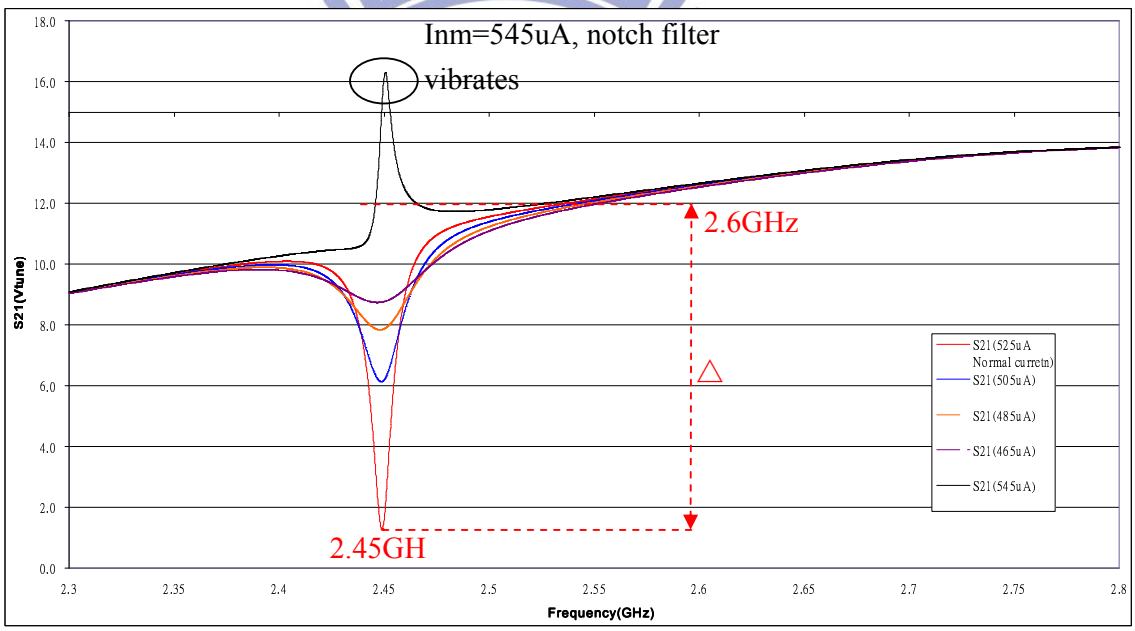

Fig 4.7 Inm (notch current) vs Notch filter Q value of WiMAX

It could be found from Fig 4.5 notch frequency could only reach 2.65GHz due to process discrepancies and uncertainties. Thus, △=13.2(2.45GHz)-2.6(2.65GHz) =10.6. (Fig 4.8). Likewise, either Q value or △ goes down with Inm, yet a peak value is observed at 830uA.

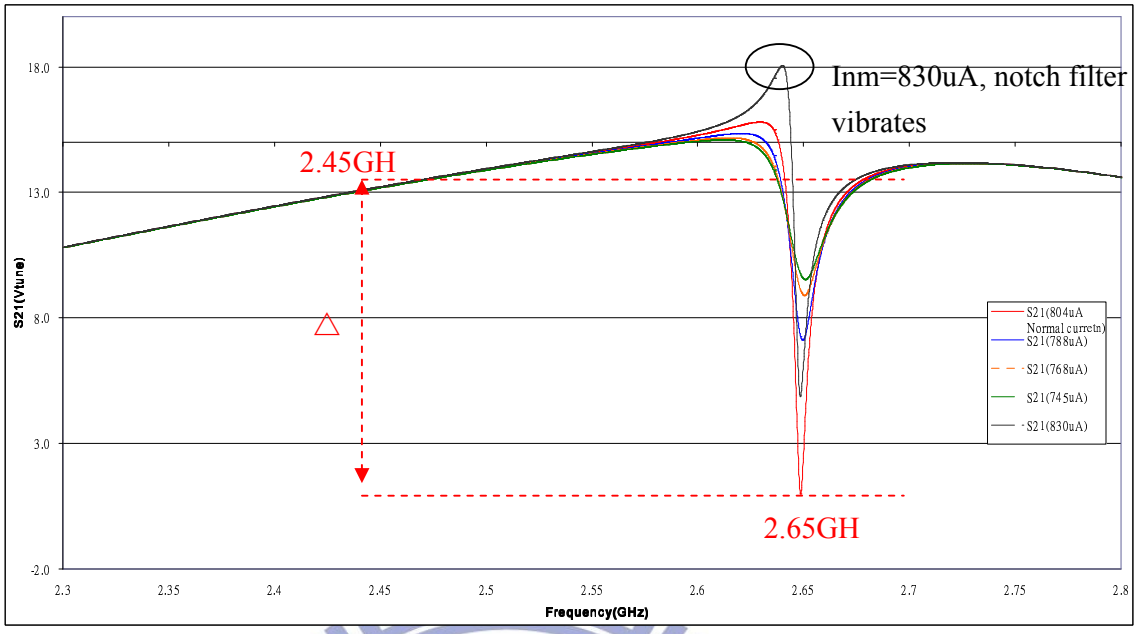

Fig 4.8 Inm (notch current) vs Notch Q value of WLAN

4.4 Measurement

WiMAX signal

Fig 4.9 Three gain modes, high gain, medium gain and low gain

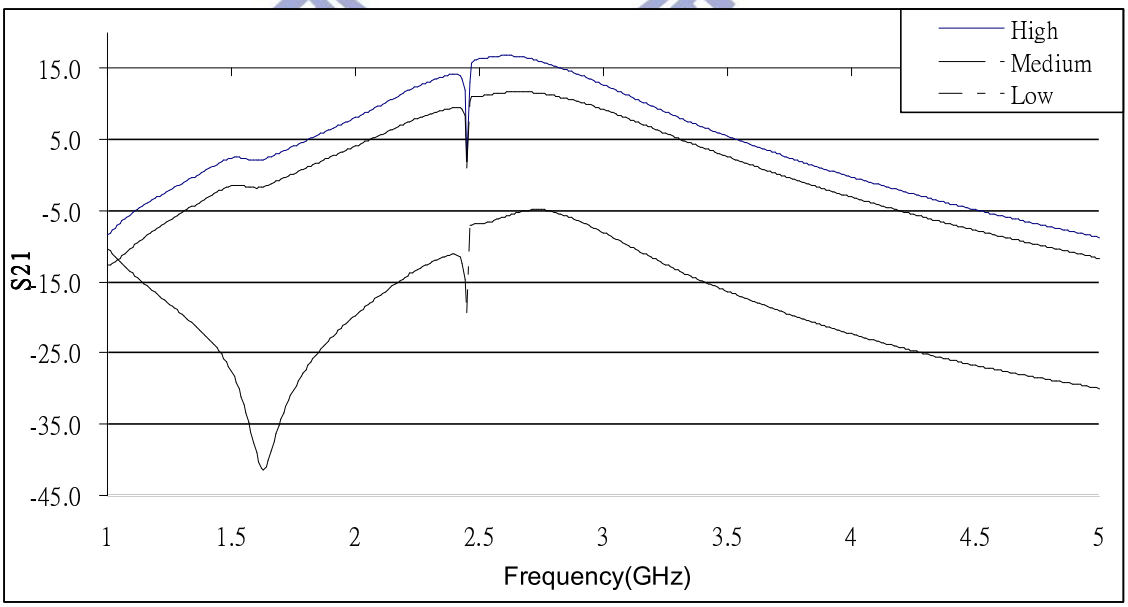

Fig 4.9 S21 measurement

Fig 4.10 shows a peak value at A caused by the passed frequency by notch filter. Thus a significantly high NF can be observed at 2.45GHz

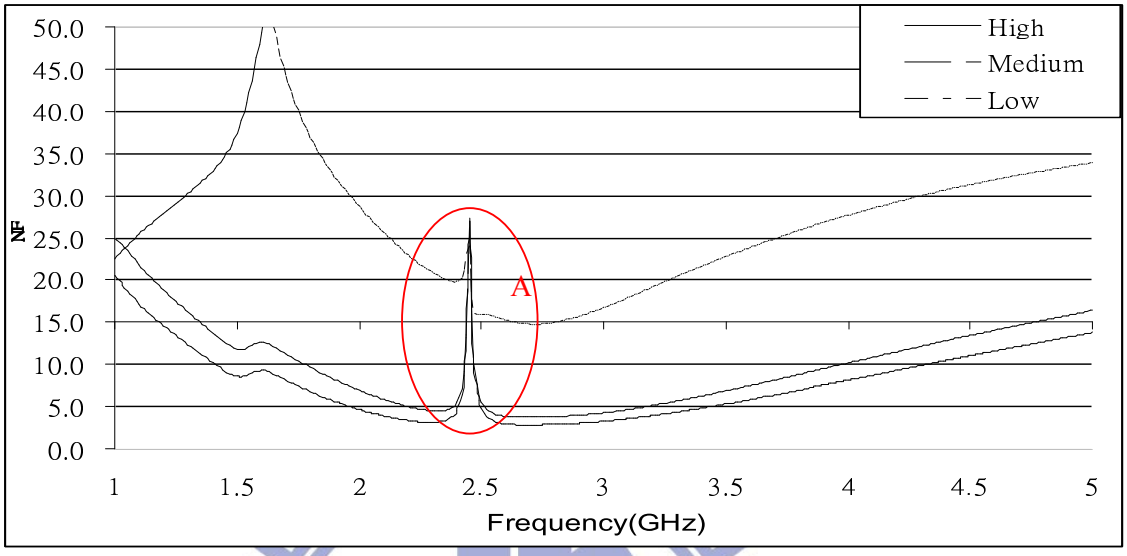

Fig 4.10 NF measurement

Fig 4.11 shows all measurements for S11are below -10dB.

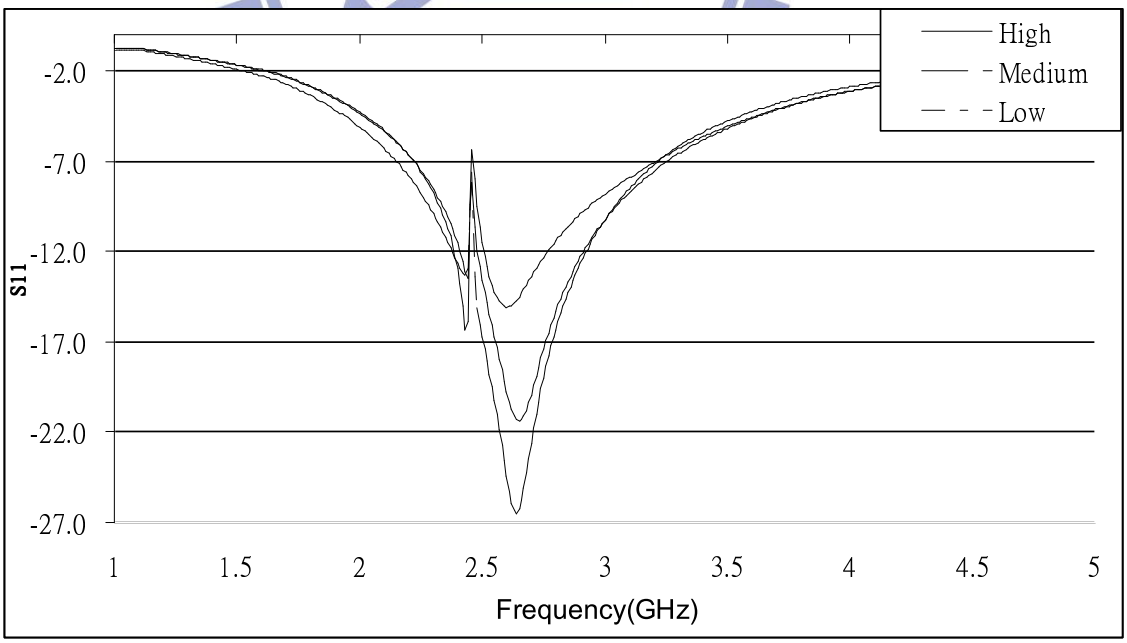

Fig 4.11 S11 measurement

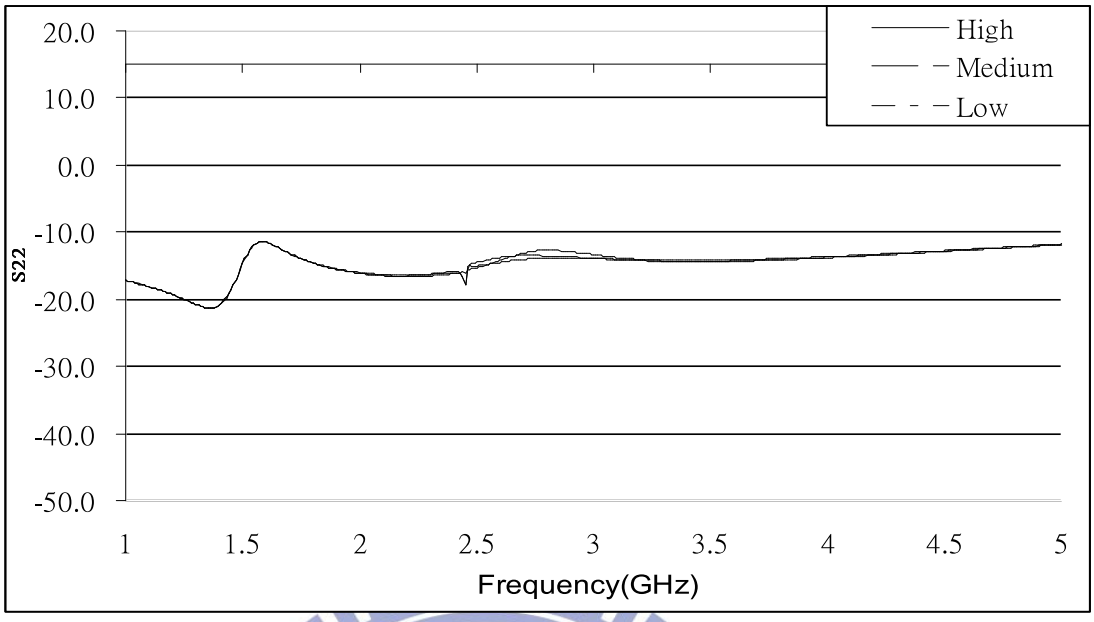

Fig 4.12 S22 measurement

It can be observed from Fig 4.13, impedance matching close to50Ω in simulation measured over 50Ω, as shown in Fig 4.13a. The reason for the might be that the section in PCB layer at RF is so long that parasites incurred affects the measurements.

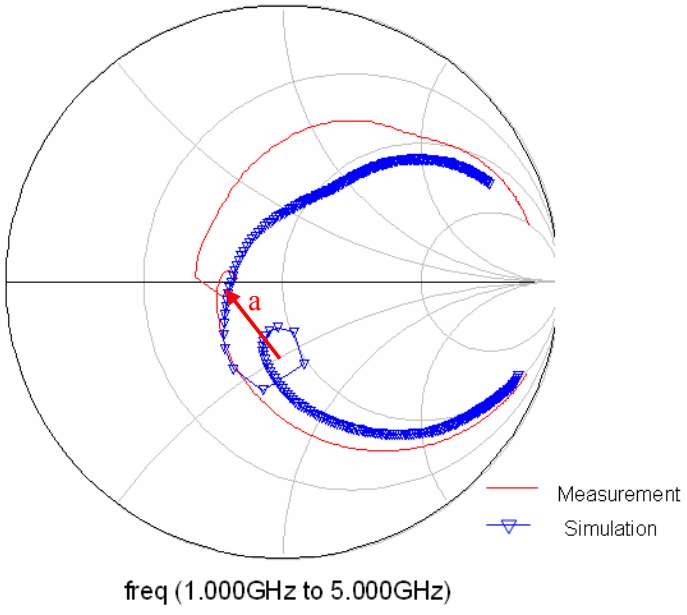

Fig 4.13 Smith chart

WLAN signal

Fig 4.14 shows the three gain modes, high gain, medium gain and low gain

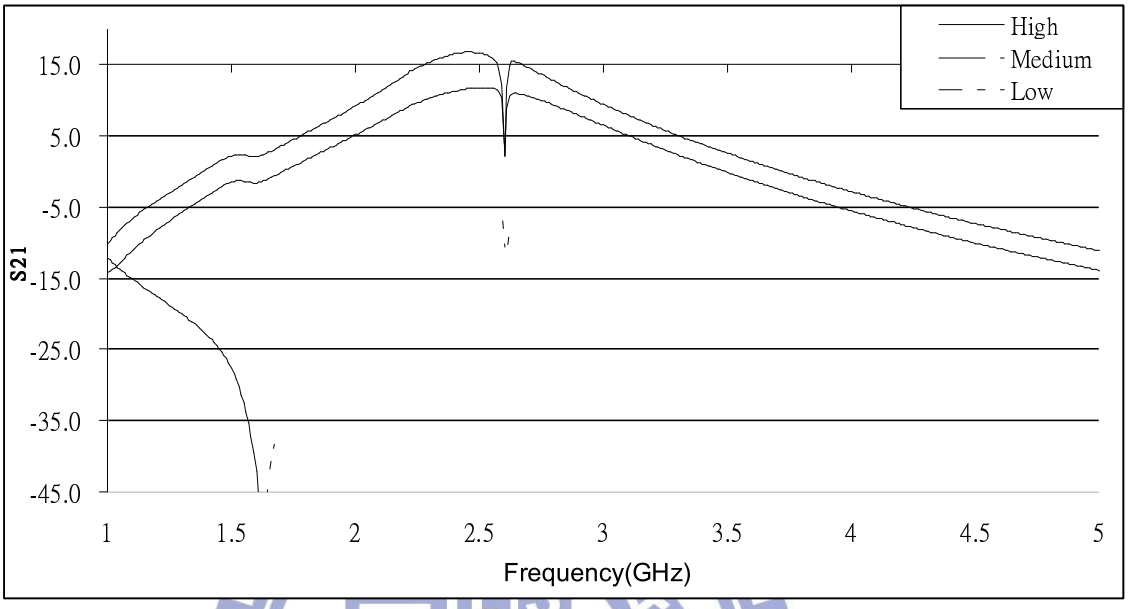

Fig 4.14 S21 measurement

Fig 4.15 shows a peak value at A is caused by the passed frequency by notch filter. Thus a significantly high NF can be observed at 2.65GHz

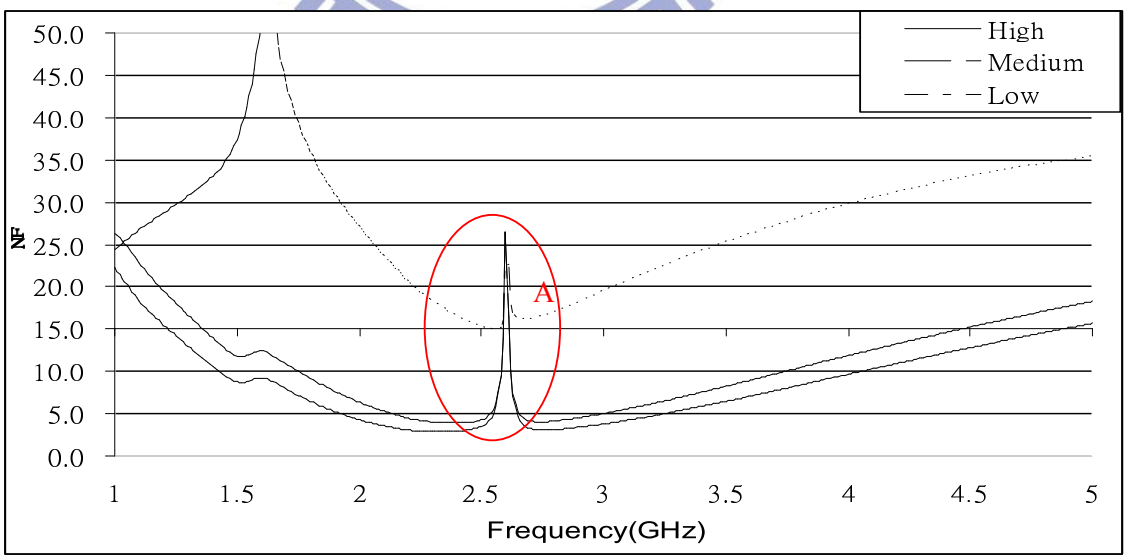

Fig 4.15 NF measurement

Fig 4.11 shows all measurements for S11are below -10dB.

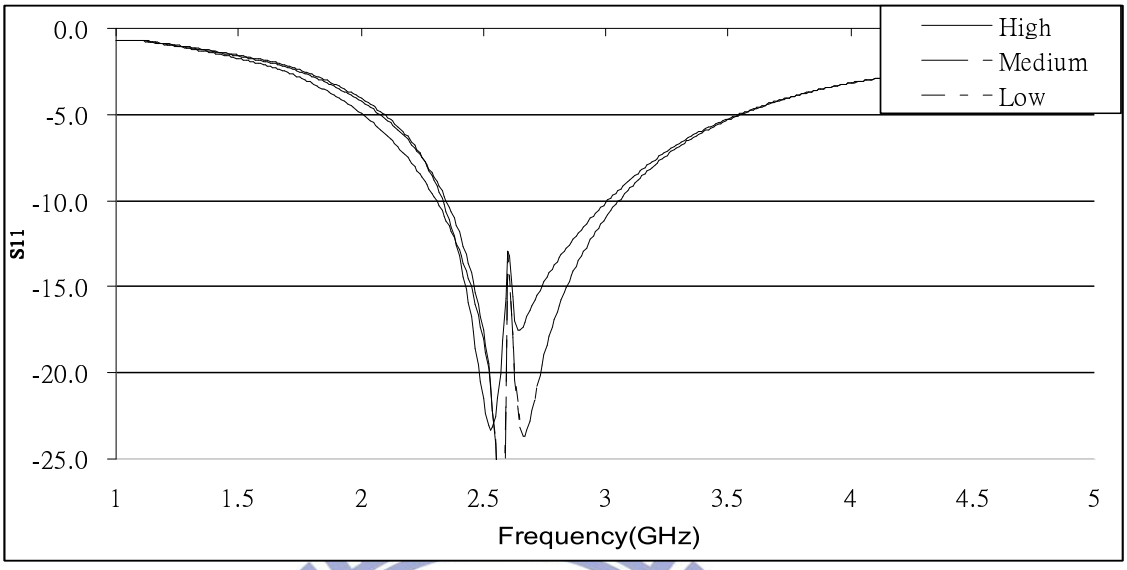

Fig 4.16 S11 measurement

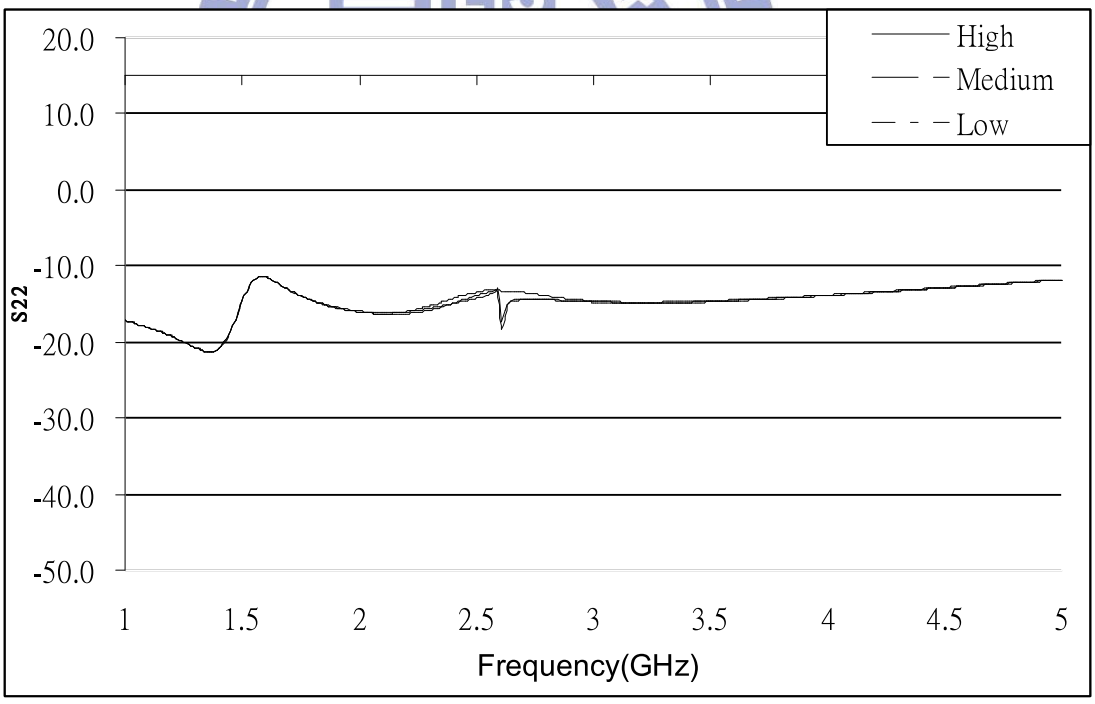

Fig 4.17 S22 measurement

It can be observed from Fig 4.18, impedance matching close to50Ω in simulation measured over 50Ω, as shown in Fig 4.18b the reason for that might be that the section in PCB layer at RF is so long that parasites incurred affects the measurements.

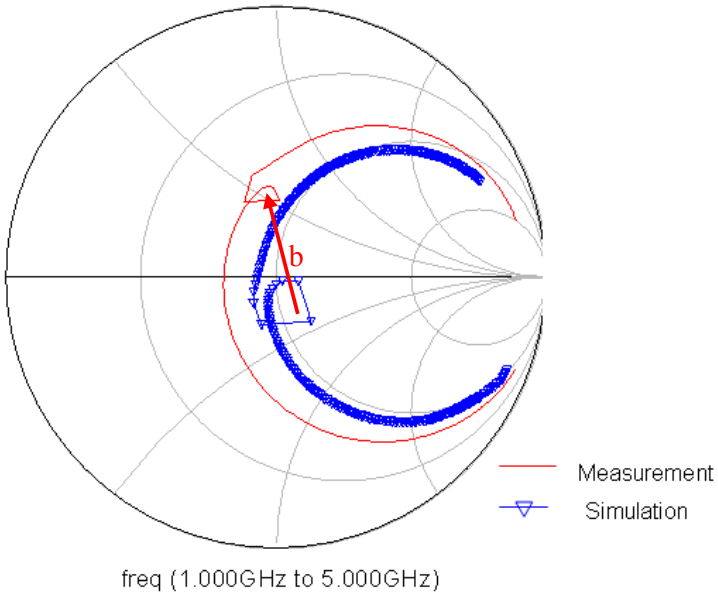

Fig 4.18 S11 smith chart

4.5 Compare Simulation and Measurement

Table 4.2 presents a significant difference between measurement and simulation due to the discrepancies in outdated process data. Initially, circuit adjustment is taken into account for active notch filter out of consideration for frequency shift. However, S21 adjustment is neglected so that S21 value of WLAN (Fig 4.4) and WiMAX (Fig 4.2) caused gain degradation due to frequency shift (Fig 4.2).

Table 4.2 Compare Simulation and Measurement

WiMAX									
	LNA with notch filter measurement			LNA with notch filter simulation			LNA simulation		
	High gain	Medium gain	Low gain	High gain	Medium gain	Low gain	High gain	Medium gain	Low gain
Parameter	0.18um CMOS Standard								
Vdd	1.8V								
S21	12.62	8.5	-15	16.9	11.6	-8	20	13	-6.6
S11	-7.83	-9.3	-9.53	-16.4	-19.7	-17.2	-15	-19.7	-21
S22	-12.18	-12.3	-12.2	-13.7	-14.5	-13.7	-15	-15	-15
NF	4.1	4.89	23.15	2.87	3.8	16.2	2.6	4.3	17.7
P1dB	-11	-9.5	-4.5	-27.5	-16	-3	-22	-16	-3
IIP3	-4.9	-2.4	-1.3	-17.9	-5.7	6	-12.4	-5.8	1.6
△	11.03	9.34	2.1	15	12.6	11.7	NA		
Power comsumption	13.8mW			13.7mW			13.86mW		

WLAN									
	LNA with notch filter measurement			LNA with notch filter simulation			LNA simulation		
	High gain	Medium gain	Low gain	High gain	Medium gain	Low gain	High gain	Medium gain	Low gain
Parameter	0.18um CMOS Standard								
Vdd	1.8V								
S21	13.2	8.9	-16.2	16.1	11.6	-5.3	19.2	12.5	-7.1
S11	-10.5	-12.4	-13.7	-15.8	-14.1	-11.7	-14.6	-15	-16
S22	-12.9	-13.8	-13	-13.8	-14.6	-13.8	-15	-15	-15
NF	4.1	5.02	24.7	2.8	3.9	16.7	2.5	4.3	18.1
P1dB	-11	-8.5	-5.5	-27.5	-15.5	-3	-21.5	-15.5	-3.5
IIP3	-3.8	-2.3	-1.7	-18	-6.9	6	-12.1	-6.9	1.1
△	10.6	8.4	6.2	13.9	9.3	6.5	NA		
Power comsumption	13.8mW			13.7mW			13.86mW		

Ref	[11]	[16]	[17]
Vdd	-	1.8	1.5
S21	-	11.8	12
S11	-18	-17.8	-35
S22	-20	-10.7	-
NF	1.5	4.95	2.4
P1dB	-16	-12	-
IIP3	-	-	-12.5
△	20 (4.25 GHz)	8.25 (1.25–1.49 GHz)	50 (10.5~11.1 GHz)
Power consumption	12	11mW	22mW

Microphotograph of Chip

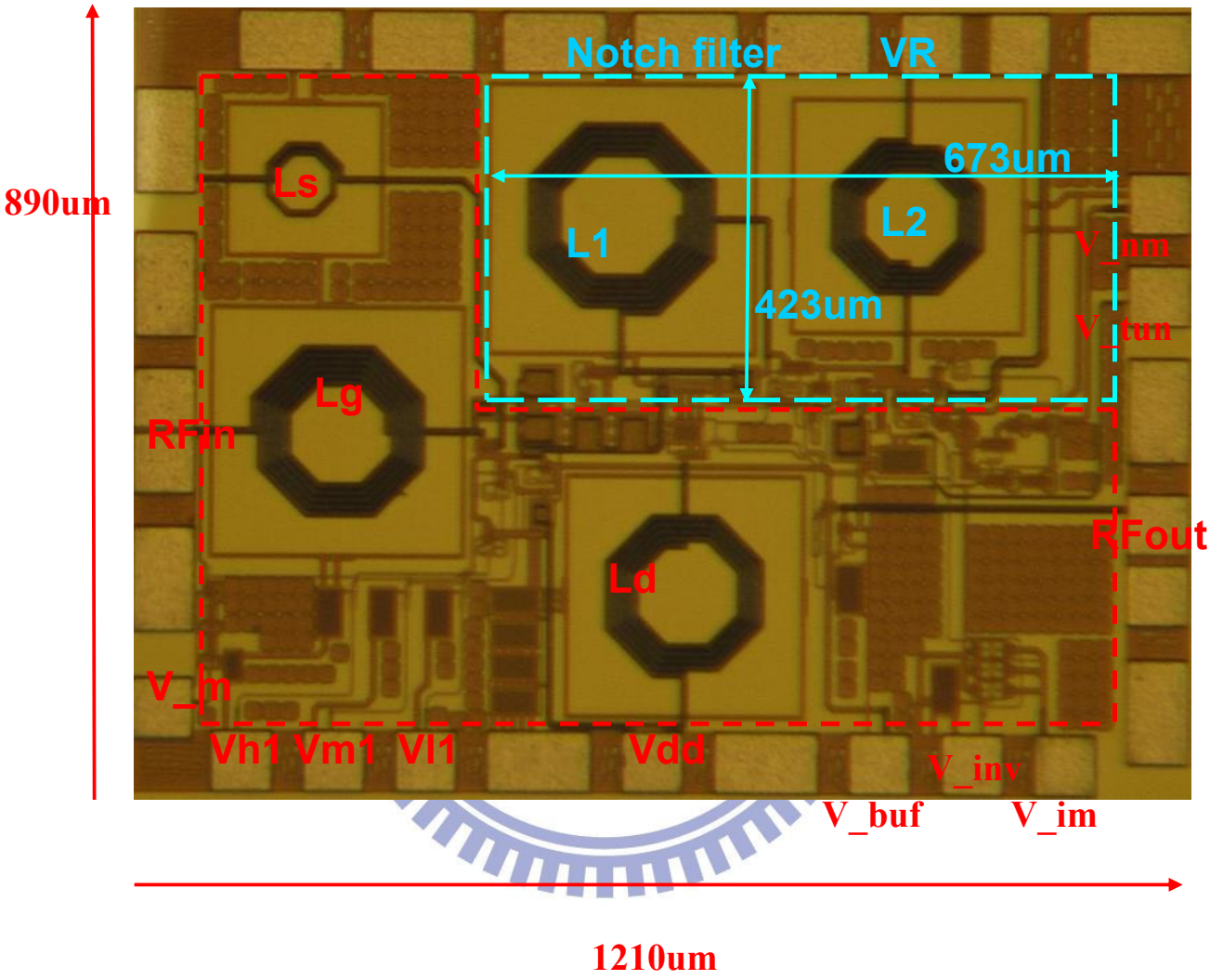

Fig 4.18 Microphotograph of LNA with active notch filter

Chapter 5

Conclusion and future work

Though comparing the measurements with simulation, a 400MHz shift toward higher frequency is found. The reason for the discrepancy is that outdated process is used in design but never cross-validated with Specter RF finally, and thus the part of design for varactor is somewhat out of place while the part for notch filter can still meet expectations due to Vtune voltage adjustment. The design in this study falls of expectation in two aspects: (1) the difference between filtered frequency and wanted frequency should be greater than 30dB, yet the measured △ is only 10dB. Therefore, more studies are needed in this aspect. (2) α (Fig 4.3) is to small to filter out noise frequency completely. Thus noise frequency might still interfere with the wanted frequency. Therefore, the above two points must be stressed in future studies.

Reference

[1] Ming-Chang SUN, Ying-Haw SHU, Nonmembers, Shing TENQCHEN, Member,and Wu-Shiung FENG, Nonmember "A One-Step Input Matching Method for Cascode CMOS Low-NoiseAmplifiers ", IEICE TRANS. ELECTRON., VOL.E88–C, NO.3 MARCH 2005

[2] Hossein Hashemi, and Ali Hajimiri," Concurrent Multiband Low-Noise Amplifiers—Theory, Design, and Applications" TRANSACTIONS ON MICROWAVE THEORY AND TECHNIQUES, VOL. 50, NO. 1, JANUARY 2002

[3] D. K. Shaeffer and T. H. Lee, " A 1.5V, 1.5GHz CMOS Low noise amplifier," IEEE Journal of Solid-State Circuit, vol 32, no.5, p.745 , May 1997

[4]T. H. Lee, The design of CMOS Radio-Frequency Integrated Circuits, Chapter 10, Cambridge.

[5] Kim, J. 4. KO, and K. Lee, "A new linearization technique for MOSFET RF amplifier using multiple gated transistors," IEEE Micmwave & Guided Wave Lett., vol. IO, no. 9, pp.371-373, Sept. 2000.

[6] V. Aparin and L. E. Larson, "Linearization of monolithic LNAs using low-frequency low-impedance input termination," Europ. Solid-State Circ. Conf., pp. 137- 140, Sept. 2003

[7] Y.S. Wang and L.-H. Lu," 5.7 GHz low-power variable-gain LNA in 0.18 lm CMOS" ELECTRONICS LETTERS 20th January 2005 Vol. 41 No. 2

[8] Air Interface for Fixed Broadband Wireless Access Systems-Amendment 2 : Medium Access Control Modifications and Additional Physical Layer Specifications for 2-11 GHz, IEEE std. 802.16a, Part 16, 2003.

[9] Keng Leong Fong, "Dual-Band High-Linearity Variable-Gain Low-Noise Amplifiers for Wireless Applications", ISSCC99 / SESSION 13 /PAPER TP 13.3

[10] Chien-Nan-Kuo，Yu-Ting-Cheng, "Low Power 3~8GHz UWB Tunable LNA Design Using SiP Technology", IEEE int. Symp. Circuit and System, 5099~5102, Japan, May 2005

[11] Trung-Kien Nguyen, Nam-Jin Oh, Choong-Yul Cha, Yong-Hun Oh, Gook-Ju Ihm, and Sang-Gug Lee, Member, IEEE "Image-Rejection CMOS Low-Noise Amplifier Design Optimization Techniques", IEEE TRANSACTIONS ON MICROWAVE THEORY AND TECHNIQUES, VOL. 53, NO. 2, FEBRUARY 2005

[12] Ching-Kuang C. Tzuang, Fellow, IEEE, Hsien-Hung Wu, Student Member, IEEE, Hsien-Shun Wu, Member, IEEE, and Johnsea Chen" CMOS Active Bandpass Filter Using Compacted Synthetic Quasi-TEM Lines at C-Band" IEEE TRANSACTIONS ON MICROWAVE THEORY AND TECHNIQUES, VOL. 54, NO. 12, DECEMBER 2006

[13] Bijoy Kuanr1, I. R. Harward1, D. L. Marvin1, T. Fal1, R. E. Camley1, D. L. Mills2, and Z. Celinski1, Member, IEEE, "High-Frequency Signal Processing Using Ferromagnetic Metals", IEEE TRANSACTIONS ON MAGNETICS, VOL. 41, NO. 10, OCTOBER 2005

[14] T.H. Lee,H. Samavati, andH. R. Rategh, "5-GHz CMOS wireless LANs," IEEE Transactions on Microwave Theory and Techniques, vol. 50, no. 1, pp. 268–280, 2002.

[15] T.-K. Nguyen, S.-K. Han and S.-G. Lee, "Ultra-low-power 2.4 GHz image-rejection low-noise amplifier", ELECTRONICS LETTERS 21st July 2005 Vol. 41 No. 15

[16] T.-K. Nguyen, N.-J. Oh, C.-Y. Cha, Y.-H. Oh, G.-J. Ihm, and S.-G. Lee, "Image-rejection CMOS low-noise amplifier design optimization techniques" IEEE Transactions on Microwave Theory and Techniques, vol. 53, no. 2, pp. 538–547, 2005.

[17] R. A. Baki and M. N. El-Gamal, "A 1.5Vmultigigahertz CMOS tunable image reject notch filter," in Proceedings of the 14th International Conference on Microelectronics (ICM '02), pp. 144–147, Beirut, Lebanon, December 2002.

[18] Byunghoo Jung, and Ramesh Harjani, "High-Frequency LC VCO Design Using Capacitive Degeneration", IEEE JOURNAL OF SOLID-STATE CIRCUITS, VOL. 39, NO. 12, DECEMBER 2004

[19] Chung-Yu. Wu, Yu Cheng, and Jeng Gong, "THE NEW CMOS 2V LOW-POWER IF FULLY DIFFERENTIAL Rm-C BANDP ASS AMPLIFIER FOR RF WIRELESS RECEIVERS", ISCAS 2000 - IEEE International Symposium on Circuits and Systems, May 28-31, 2000, Geneva, Switzerland.